Energy & Buildings 366 (2026) 117716

Contents lists available at ScienceDirect

Energy & Buildings

journal homepage: www.elsevier.com/locate/enb

Integrating operational and embodied CO_2 emissions: a comprehensive life cycle approach to buildings' system-installations retrofitting with a new indicator

Elżbieta Broniewicz [a], Piotr Rynkowski [a], Beata Sadowska [a], Anna Justyna Werner-Juszczuk [a], Eugenia Rossi di Schio [b], Paolo Valdiserri [b], Maciej Kłopotowski [a], Bożena Babiarz [c], Alicja Siuta-Olcha [d], Tomasz Cholewa [d], Dorota Anna Krawczyk [a,*]

[a] Department of Sustainable Construction and Building Systems, Faculty of Civil Engineering and Environmental Sciences, Białystok University of Technology, Wiejska 45A, 15-351 Białystok, Poland
[b] Alma Mater Studiorum – University of Bologna, Department of Industrial Engineering DIN. Viale Risorgimento 2, 40136 Bologna, Italy
[c] Faculty of Civil and Environmental Engineering and Architecture, Rzeszów University of Technology, Powstańców Warszawy Street 12, 35-959 Rzeszów, Poland
[d] Faculty of Environmental Engineering and Energy, Lublin University of Technology, Nadbystrzycka 40B, 20-618 Lublin, Poland

ARTICLE INFO

Keywords:
CO_2 Emission
Heat Consumption
LCA
Retrofitting
HVAC Systems
RES integration

ABSTRACT

In the context of increasing energy efficiency requirements and climate neutrality goals for the building sector, evaluating comprehensive retrofit strategies for existing public buildings has become a key research and policy priority. This study presents a comprehensive life-cycle assessment (LCA) of energy retrofit strategy for a 40-year-old public kindergarten in Poland. The analysis evaluates twelve cumulative retrofit scenarios encompassing both building envelope enhancements and technical system upgrades. Envelope improvements include stepwise insulation of the entrance canopy, external walls, flat roof, basement walls, and replacement of windows and doors. Technical system interventions span the retrofitting of domestic hot water (DHW) and central heating (CH) systems, replacement of the heat source with an air-source heat pump (ASHP), and integration of rooftop photovoltaic (PV) panels and battery energy storage. Each scenario's impact on energy demand and CO_2 emissions was quantified over a 30-year service life using averaged local climate data. Results demonstrate that envelope retrofits can achieve up to 60% reduction in final energy demand, while technical upgrades, particularly the transition to a high-efficiency ASHP and renewable electricity integration, can yield over 90% total energy savings. A novel indicator was introduced to assess CO_2 reduction efficiency per unit of energy saved. While the LCA followed standard methodologies by focusing on product and operational stages, the study acknowledges limitations related to the exclusion of demolition and waste phases, which may underestimate total environmental impacts. Thus, there is a need for future studies in this area.

1. Introduction

Improving the energy efficiency of buildings is one of the key pillars of the European Green Deal (EGD), which aims to achieve climate neutrality by 2050 [1] (Directive 2023/1791). The building sector plays a fundamental role in this transition, as it accounts for approximately 40% of energy consumption and 36% of greenhouse gas GHG emissions within the European Union [2]. A crucial component of this process is the shift toward renewable energy sources, which is essential to achieving the target of reducing GHG emissions by at least 55% by 2030 compared to 1990 levels [3]. To support this objective, the "Retrotiffing Wave" strategy under the EGD promotes the retrotiffing of public buildings such as schools, hospitals, and administrative facilities [4]. One of the core principles of the Retrotiffing Wave is to reduce emissions throughout the entire life cycle of buildings and to utilize on-site renewable energy sources.

Although, carbon dioxide removal (CDR) technologies have been assigned significant greenhouse gas removal potentials in part of studies, the other research highlights that their environmental assessments remain immature and often unreliable from an LCA standpoint [5]. This

* Corresponding author.
E-mail address: d.krawczyk@pb.edu.pl (D.A. Krawczyk).

https://doi.org/10.1016/j.enbuild.2026.117716
Received 12 October 2025; Received in revised form 30 April 2026; Accepted 26 May 2026
Available online 28 May 2026

reinforces the critical importance of advancing near-term mitigation through building retrofits, whose benefits are well-quantified and actionable. In this context, Famiglietti et al. [6] proposed a new tool helpful in the environmental evaluation of buildings and tested it on approximately 81,000 building units in Milan, concluding that the space heating remains the main contributor to the climate change impact.

Many studies have addressed various aspects of the environmental performance of building retrofit strategies. For example, Dylewski and Adamczyk [7] focused on a comprehensive assessment of the environmental impact of thermal insulation in buildings, specifically within the context of Polish climatic and construction conditions. Their LCA aimed to determine the ecological benefits resulting from the investment in external wall insulation. The study examined different types of thermal insulation materials and heat sources. The findings indicated that thermal insulation investments were environmentally beneficial in all scenarios analyzed, with the highest environmental gains observed when using eco-fibber as the insulation material. Makhmudov et al. [8] conducted an LCA of multi-family residential buildings focused exclusively on building envelope improvements, without modifications to the heating system. The study found that the retrofitting process led to a 13.5% reduction in GHG emissions, despite an initial increased due to the production of insulation materials. Over a 60-year life cycle, the total CO_2 emissions were reduced by 24%, equivalent to 43.2 tonnes of CO_2.

Studies on heritage buildings also highlight the potential of fabric improvements. González-Prieto et al. [9] investigated the environmental impact of retrofitting a 20th-century heritage building in Spain, analyzing both the retrotiffing and operational phases. Their LCA covered various retrofit scenarios, including installation upgrades, improved thermal insulation, and the use of advanced technologies. The study also accounted for the influence of energy sector decarbonization on the building's environmental performance over time. The authors concluded that well-designed retrofitting of historic buildings, particularly those incorporating renewable energy sources, could significantly reduce their environmental footprint.

Several studies have been conducted to evaluate combined retrofit strategies involving both envelope and system upgrades. A subsequent study [10] examined three levels of thermal retrofitting in single-family buildings: (1) retrotiffing or replacement of the heat source, (2) heat source upgrade combined with window replacement or façade insulation, and (3) comprehensive retrotiffing incorporating renewable energy sources. In all scenarios, significant environmental benefits were achieved. However, the authors emphasized that these benefits are accompanied by considerable economic costs.

Similarly, Asdrubali et al. [11] analyzed the retrofitting of a public school in northern Italy. The analysis considered scenarios involving the insulation of external partitions and upgrades to technical systems. The results showed that energy demand could be reduced by 55% to 74%, depending on the scenario. Reductions in total primary energy use and overall CO_2 emissions ranged from 30% to 44%. Conversely, Mastrucci et al. [12] proposed a spatio-temporal LCA framework to assess retrotiffingscenarios of urban housing stocks, including e.g., energy demand modelling and product-based LCA, to conclude that the retrotiffingstage represented 4%–16% of the carbon footprint in the residual service life of existing buildings.

Research comparing conventional retrofits with high-performance standards indicates notable differences. Sierra-Pérez et al. [13] reported 20% higher energy savings for Passivhaus renovations in comparison to a conventional one, while the ratio of embodied energy and environmental impacts was the opposite.

A comparative analysis of two residential buildings demonstrated that the embodied emissions component slightly exceeded the operational emissions in the case of a Belgian passive house, whereas the Australian house showed a predominance of operational emissions [14].

Several reviews highlight methodological gaps in existing retrofit-LCA studies. Leichter and Piccardo [15] reviewed 44 previous studies and concluded that the majority of them primarily focused on the operational phase of buildings and their energy consumption. Similarly, Vilches et al. [16] observed that only 30% of the analyzed studies included heating or cooling systems in their assessments, while domestic hot water (DHW) systems were considered in the majority (70%) of the cases. As suggested by Fahlstedt et. al [17], emphasized the importance of accounting for a changing carbon content of future electricity mixes, which can significantly influence LCA conclusions. What is more, authors noted the need for common baselines for retrotiffingprojects and claimed that more effort was needed to define how the concept of 'major renovations' from energy efficiency measures can bridge with renovation-LCA.

The aim of the paper is to evaluate the impact of several retrofitting scenarios applied to the case study building on changes in CO_2 emissions and to identify which intervention is the most energy- and environmentally efficient. To support this assessment, a novel indicator is proposed that quantifies the CO_2 emissions associated with each retrotiffing strategy, expressed per 1 GJ of energy saved as a result of the intervention.

Existing metrics, such as "emissions intensity", "emission factor" or "CO_2 intensity of energy", are commonly used to compare fuels, energy sectors or national energy systems, by representing the amount of carbon dioxide emitted relative to the useful energy content of an energy carrier. These indicators help to assess the carbon efficiency of energy systems. In practical applications, emission intensity values are used to benchmark decarbonization progress across sectors and to support the formulation of emission reduction strategies. Lower values are interpreted as an indicator of cleaner or more efficient energy use (Greenhouse Gas Emissions from Fossil Fuel Fired Power Generation Systems, European Commission Joint Research Centre, Institute For Advanced Materials).

In building-related LCA studies, environmental impacts are commonly expressed using indicators such as Global Warming Potential (GWP), cumulative energy demand, embodied energy, or various emission factors quantifying CO_2 intensity per unit of delivered energy. These metrics are widely applied to assess materials, technologies, and energy carriers. However, they offer limited insight into the relationship between the embodied impacts of a retrofit measure and the operational energy savings it delivers over time. Existing indicators are typically defined at the system or fuel level, making them less suitable for evaluating building-scale interventions, where the balance between embodied and operational impacts is critical for determining the actual mitigation potential.

To address this limitation, the present study introduces a novel indicator that normalises the CO_2 emissions associated with each retrofit scenario by the energy savings achieved in the case study building, expressed per 1 GJ of energy conserved. This formulation enables a direct comparison of alternative retrofit strategies within a consistent decision-making framework and provides a more transparent assessment of their relative environmental efficiency.

Existing indicators such as Life Cycle Global Warming Potential (GWP) and Whole-Life Carbon (WLC) refer to greenhouse gas emissions from the entire life cycle of a building. The need to integrate energy and CO2 into a single set of indicators is evident. Current environmental indicators indicate a lack of a uniform approach to linking energy quality, such as the share of renewable energy sources, seasonality, and heating system efficiency, with emissions. The proposed indicator fills this gap and can be used in engineering studies such as energy audits and energy performance certificates. It is very clear and logical. It will allow for the determination of energy demand and emissions for various buildings, similarly to the case with heating demand indicators.

2. Methodology

The first step of the analysis involved selection of a representative kindergarten building that would allow the results to be extrapolated to preschool buildings commonly found in Eastern Europe. The

justification for choosing a particular kindergarten is presented in the section 3. The overall research framework is presented in Fig. 1.

Subsequently, data were collected on the current condition of the facility, focusing on the quality of the building envelope and the state of its technical systems – particularly the domestic hot water (DHW), central heating (CH), ventilation systems, and sources of heat and electricity. Energy consumption data for both electricity and heat were obtained for the years 2022–2024 based on invoices from energy providers (section 4).

Following the assessment of the building's current condition, 12 retrofit scenarios were proposed (section 5) based on energy audit. These included improvements to the thermal performance of the building envelope, retrotiffing of the DHW and CH systems, and upgrades to the sources of heat and electricity, by use of renewable energy sources (RES). For each retrofit scenario, calculations were performed to determine the impact of the proposed changes on the building's overall energy demand (methodology presented in sections 2.1 for scenarios concerning building envelope and CH and DHW systems and section 2.2 for scenarios with RES) and reduction of CO_2 emissions. The final stage of the methodology involved conducting a Life Cycle Assessment (LCA) for each of the 12 scenarios, considering all life cycle stages – i.e., cradle-to-grave (section 2.3). Based on the results, a new indicator, the CO_2 reduction efficiency of retrotiffing projects, has been defined, with the aim of assisting in the selection of the optimal retrotiffing scenario for a building.

2.1. Heat demand calculations

To determine the heat demand for the building in its current state and for proposed retrofit scenario (related to the building envelope and CH, DHW systems), the methodology for conducting energy audits of buildings was applied [18], which is legally mandated in Poland for evaluating the justification of thermal retrotiffing easures. The annual usable energy demand for space heating $Q_{H.nd}$ (Fig. 2), and for hot water preparation Q_W was calculated according to the methodology presented in [19], in force in Poland since 27 February 2015.

The final formula for calculating the annual usable energy demand for space heating, $Q_{H.nd,}$ has the form of (1):

$$Q_{H,nd} = \sum \left(A_i U_i + \sum l_i \Psi_i \right) b_{tr,i} (\theta_{int} - \theta_{e,n}) t_{m,n} + \\ + \rho_a c_a \sum b_{ve} V_{ve} (\theta_{int} - \theta_{e,n}) t_{m,n} - \eta_{h,gn,n} \left(\sum C_i A_{oi} l_i F_{sh,gl} F_{sh} g_{gl} + q_{int} A_f t_{m,n} \right) \quad (1)$$

In addition to the data presented in Fig. 2, the formula (1) includes other variables from methodology [19]: the reduction factors for the adjacent unheated spaces ($b_{tr,i}$, b_{ve}), the number of hours in a month ($t_{m,n}$), the dimensionless gain utilization factor in the heated zone s in the *n-th* month of the year ($\eta_{H,gn,n}$).

The usable energy demand for hot water preparation Q_W depends on unit daily demand for domestic hot water (V_{wi}) in relation to the usable area, specific heat of water (c_w), density of water (ρ_w), hot water temperature in a draw-off tap (θ_{cw}), temperature of cold water (θ_{co}), correction coefficient due to breaks in use (k_R) and number of days in a year (t_R) (2):

$$Q_w = V_{wi} A_f c_w \rho_w (\theta_{cw} - \theta_{co}) k_R t_R \quad (2)$$

The values of cold and hot water temperature were determined in accordance with the Polish standard and are respectively 10°C and 55°C. In kindergarten facilities demand for DHW (V_{wi}) is 0.8 $dm^3/(m^2 \cdot day)$, and the correction coefficient (k_R) is equal to 0.55, due to the high unevenness of water consumption.

Based on the values of usable energy demand (EU), the final energy (EF) demand of CH and DHW systems can be calculated from formula (3)

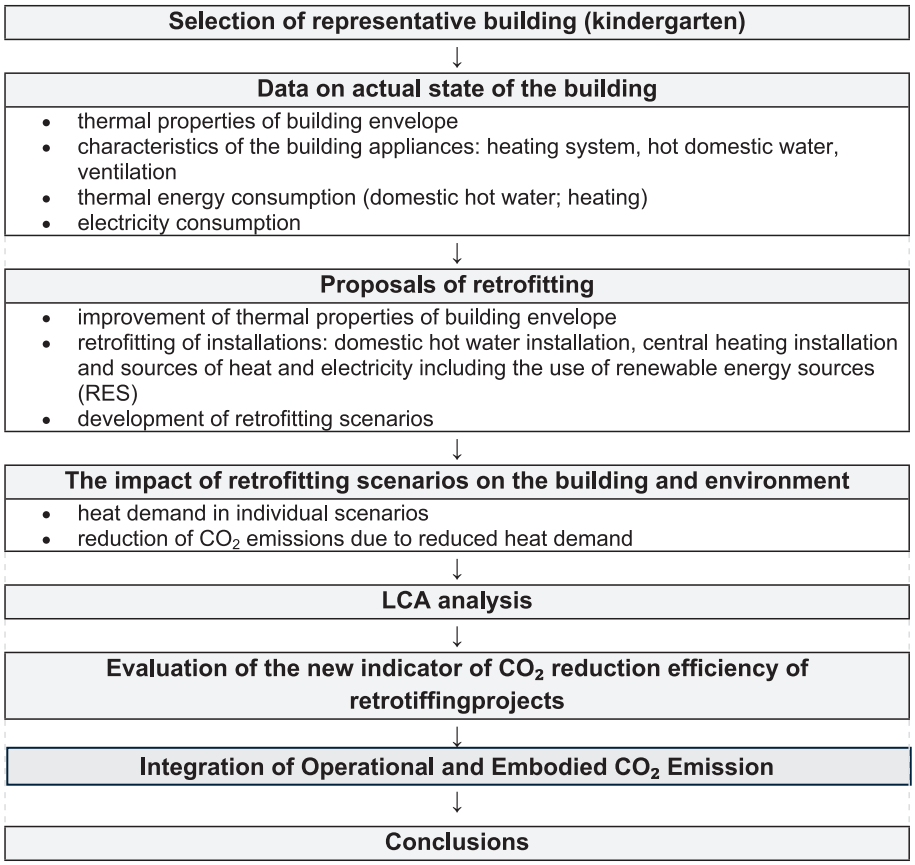

Fig. 1. Research scheme.

Annual usable energy demand for space heating $Q_{H.nd}$, kWh/month

- determination of number of heated zones n
- determination of the average indoor temperature (θ_{int}) of heated zones, °C
- determination of the average outdoor temperature ($\theta_{e,n}$) in the *n-th* month of the year in the building location, °C

=

The total amount of heat transferred from the heated zone in the *n-th* month of the year $Q_{tr,s,n}$

- heat loss through external walls
- heat loss through internal partitions to unheated rooms
- heat loss to the ground

heat transfer losses	heat losses through linear thermal bridges
- the area of element i of the building envelope (A_i), m^2 - the heat transfer coefficient of element i of the building envelope (U_i), W/m^{2}K	- length of the thermal bridge (l_i), m - the linear heat transfer coefficient (ψ_l), W/mK

+

The total amount of heat transferred from the heated zone via ventilation in the *n-th* month of the year $Q_{ve,s,n}$

- the average airflow rate through the heated space (V_{ve}), m^3/s
- the heat capacity of air per volume ($\rho_a c_a$), 1200 J/(m^{3}K)
- average outdoor temperature ($\theta_{e,n}$) in the n-th month of the year, °C
- average indoor temperature (θ_{int}), °C

+

Monthly heat gains from solar radiation through windows, balcony doors and other glazed surfaces $Q_{sol,H}$

- surface area of window or door opening (A_{oi}), m^2
- the share of glass plane surface area to the total area of the window (C_i),-
- average solar radiation in the considered month on the plane in which there is a window (I_i) (includes the coordinates, based on the building location), kWh/(m^2·month)
- window/door shadings for movable devices shading - blinds, roller blinds (the reduction factor ($F_{sh,gl}$)), -
- shading from the external envelope- external walls (the reducing factor due (F_{sh})), -
- the total solar energy transmittance factor of the transparent part of the element (g_{gl})

+

Monthly internal heat gains $Q_{int,H}$

- the heat flow from users and devices (q_{int}) according to [19] (depends on the type of the building – residential, public utility, industrial), W/m^2
- usable heated area of building (A_f), m^2

Fig. 2. Scheme of calculations of annual usable energy demand for space heating $Q_{H.nd}$ (based on [19]).

[19]:

$EF = EU/\eta$ (3).

where η denotes the total efficiency of the CH or DHW system.

2.2. Retrotiffing of heat and electricity source

The study included an analysis of the potential to replace the existing heat and electricity sources with systems based on renewable energy sources (RES). For this purpose, the authors applied a previously developed methodology for simplified estimations of the effects of RES integration, which was presented in detail in the paper [20].

An updated version of this methodology [20], adapted to the specific needs of the present analysis, is illustrated in Fig. 3.

This method enables the assessment of renewable energy integration potential, taking into account the building's specific heating and electricity demands. It is based on a methodology for determining the building's usable (EU) and final (EF) energy demand [19] (section 2.1). A key element is the knowledge of the overall efficiency of the building's heating (CH) and domestic hot water (DHW) systems before and after renovation, what enables the calculation of the final (EF) energy based the value of usable (EU) energy. The overall efficiency of CH and DHW systems is the product of heat generation efficiency by the source, distribution, usage, and accumulation efficiencies. These efficiencies were determined based on an on-site inspection (building condition before retrotiffing) and the scope of the proposed retrotiffing of the CH and DHW systems, based on the guidelines provided in [19].

The usable energy demand for CH was calculated using the monthly balance method, in accordance with Polish methodology (Fig. 2 and

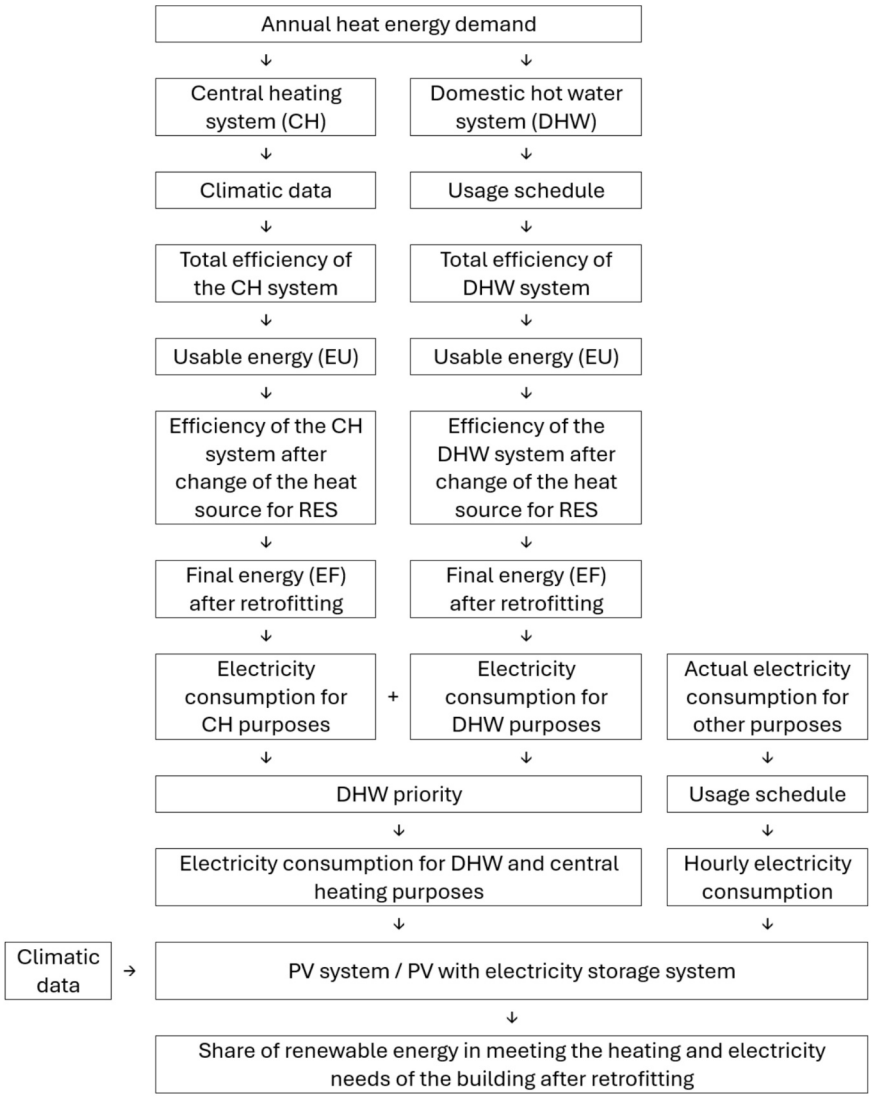

Fig. 3. Scheme of methodology [20].

section 2.1) [19]. Taking into account the outdoor temperature for each hour of a given month, the monthly usable energy demand was divided into each hour of the month to enable the RES analysis, which was carried out on an hourly basis.

The combination of the monthly and hourly methods results from the application of the methodology contained in [18]. The Polish regulation used to select optimal projects for the analyzed kindergarten requires the use of the monthly method. In this paper, the energy calculations were performed using the Audytor OZC software using averaged climatic data developed specifically for energy performance analyses for the location of Bialystok, Poland [21]. The software uses monthly methods. For renewable energy purposes, this method is unacceptable. Therefore, for the assumed data on the heat and electricity demand for the building's heating, the hourly method was used for renewable energy purposes. It should be added that work is currently underway to introduce the hourly method, primarily due to cooperation with renewable energy sources, but it is not currently implemented in Polish legislation.

For the analysis of outdoor air temperature, the calculations were performed using averaged climatic data developed specifically for energy performance assessments for the building location (Bialystok, Poland) [21].

Because the usable energy demand does not change when the heat source is modernized, and the efficiency of the CH and DHW systems after retrotiffing is known, the final energy demand after retrotiffing can be calculated. To determine the efficiency of the CH the technical data of the selected devices was used, i.e., heat pumps, and their operating characteristics: the coefficient of performance (COP), the heating capacity, and its electricity consumption, determined for operating parameters of the CH installation (i.e., supply temperature). Also, the thermal characteristics of the heat source from which the pump extracts energy was considered. The result of the calculations was the heat pump's electrical energy demand for CH and DHW preparation in the building.

The methodology (Fig. 3) allows for the assessment of the use of photovoltaic (PV) panels together with energy storage systems to cover the building's electricity demand. This requires selecting devices, that meet buildings' requirements, and defining their technical parameters, including storage capacity, PV panel surface area, efficiency, rated power output, and the annual PV efficiency degradation rate. Grid-connected (on-grid) photovoltaic systems was considered. Electricity consumption for other end uses, such as cooking and lighting, was considered in the analysis, based on actual measured data. Solar radiation data were obtained from [22]. Taking into account the size and configuration of the PV system, as well as the building's location and solar exposure, the potential electricity yield was estimated. This allowed for an assessment of the extent to which the PV system can meet

the building's electricity demand.

In calculations the actual building operation schedule was considered to determine the thermal and electrical energy demand throughout the day and year. Because the method relies the technical specifications of the RES equipment, it allows for a precise assessment of the RES integration potential and the degree to which the RES can meet the building's thermal and electrical energy demand.

In this paper, the energy calculations were performed using the Audytor OZC software using averaged climatic data developed specifically for energy performance analyses for the location of Bialystok, Poland [21]. In order to verify the correctness of the input data used for calculations, the results were compared with heat consumption. The use of averaged long-term conditions is necessary, as the subsequent stage involves performing a Life Cycle Assessment (LCA) that considers the service life of the building, its components, and technical systems. The basis for the calculations included data from energy audits regarding the thermal energy demand for space heating and domestic hot water (DHW) preparation. Information on electricity consumption was taken from utility bills for the years 2022–2024. Grid-connected (on-grid) photovoltaic systems is planned. To reduce the degree of utilization of electricity energy from the power grid, the use of an electricity storage facility is proposed.

2.3. Life cycle assessment (LCA)

The Life Cycle Assessment was carried out in accordance with the guidelines of ISO 14040:2006 + A1:2020 [23] and ISO 14044:2006 + A2:2020 [24], using the LCA for Experts software from Sphera Solutions (v.10.9.3.0). The functional unit adopted for the analysis was defined as the total scope of thermal retrotiffing necessary to achieve the assumed energy goals. Carbon dioxide (CO_2) emission was selected as the environmental impact indicator and Integrating Operational and Embodied CO_2 Emissions were presented. Carbon dioxide (CO_2) emission was selected as the environmental impact indicator, and both operational and embodied CO_2 emissions were integrated in the analysis. CO_2 was chosen because operational emissions could be calculated using official governmental data on the Polish energy mix. Data necessary to determine CO_2e emissions were not available; therefore, CO_2 was used as the primary indicator.

3. Selection of a case study building

This study was conducted in Bialystok, a city located in northeastern Poland. Ultimately, Public Kindergarten No. 68, was selected for analysis (Fig. 4). The building was constructed in 1984 and it represents a group of kindergartens with the most favourable spatial characteristics, as classified by Krawczyk et al. [20,24]. The usable floor area is estimated as 1,159.55 m^2, while its heated volume: 3,385.9 m^3. The building features a cuboidal form with a flat roof, and its facade is articulated by continuous rows of identical large windows. Detailed information is presented in Annex A.

4. Current state of the building

4.1. Thermal properties of building envelope elements

Heat transfer coefficients (*U*-values) of individual building components of the analyzed kindergarten in their current (pre-retrofit) condition are presented in the Table 1.

U_{Cmax} values are presented in accordance with Polish building regulations [27], which are representative for Cold Temperate Climate

Table 1
Heat transfer coefficients (U-values) of building envelope elements – current state [26].

Building element	U [W/m^{2}K]	U_{Cmax} [W/m^{2}K] [27]
External walls		
– above-ground storeys	1.16	0.20
– basement walls above ground level	1.50	
– basement walls below ground level	0.87	
Roof / flat roof / ceiling under unheated attic or above open passageways	0.58	0.15
Windows and balcony doors	2.00	0.90
External doors and gates	3.00	1.30
Canopy over the entrance vestibule *(ti = 8°C)*	3.95	0.30
Ground slab	0.44	0.30

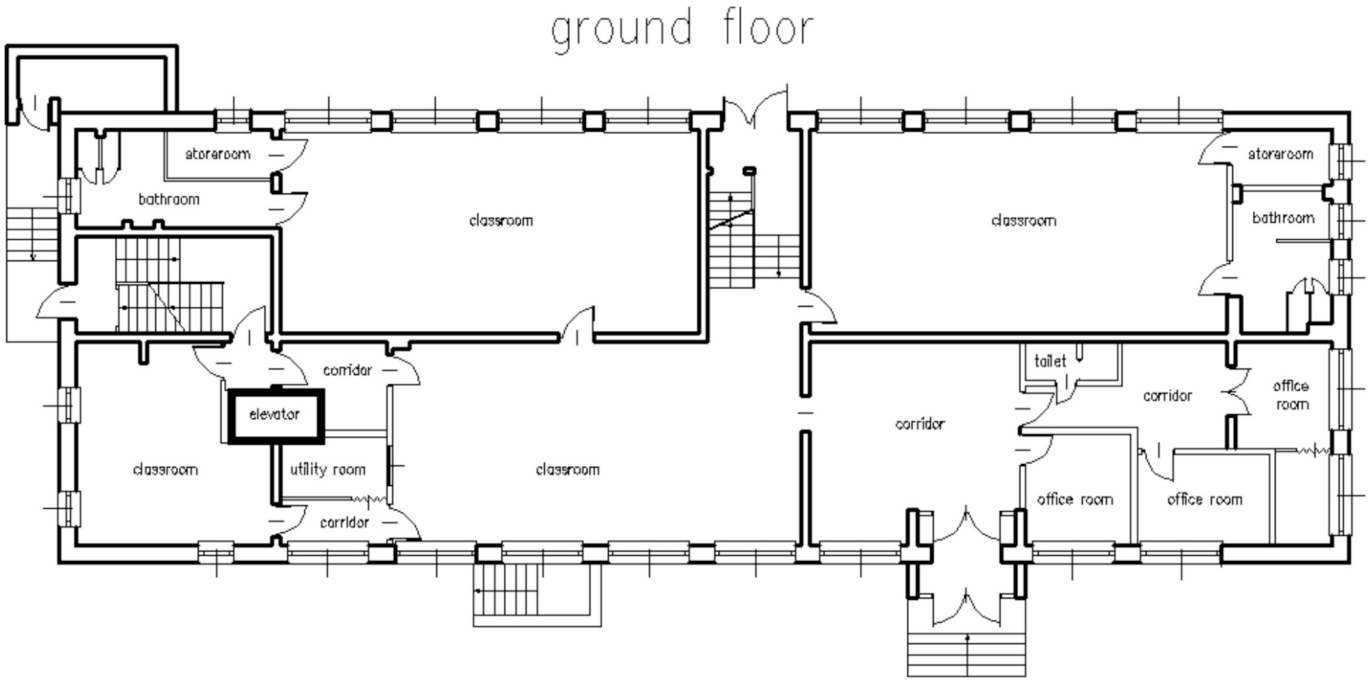

Fig. 4. Ground floor plan of the building considered in the analyses.

Zone [28]. The proposed retrofitting strategies were designed to achieve U values lower than the corresponding $U_{Cmax.}$ limits. The only exception is the ground slab in heated rooms, which has a U-value of 0.44 [W/m^{2}K]). Although this value does not meet the requirements of thermal protection, the isolation of the slab was not included in the retrofit measures due to technical constraints- specifically, the need to maintain the existing room height.

4.2. Ventilation system

The building is equipped with a gravity (natural) ventilation system, except for the kitchen, where mechanical exhaust ventilation is installed. In the remaining rooms of the preschool, air exhaust is provided by gravity ventilation ducts located in children's activity rooms, bathrooms, the kitchen, and corridors. Air supply is achieved through window leakage and by manually opening windows and doors. There is no possibility of controlling the airflow rate of the ventilation system. The air exchange rate per hour (ACH) in the building was determined based on the data contained in [19], in accordance with the methodology for preparing energy audits. According to the recommendations 1 ACH was assumed in the utility rooms, 0.3 ACH in the vestibule (with an area of 5.8 m^2), and 3.2 ACH in the rooms with mechanical exhaust ventilation (89.06 m^2 of the kindergarten).

4.3. Heating and domestic hot water systems

The current heat source in the analyzed kindergarten is a district heating substation supplied by the municipal district heating network. It provides heat for both the CH and DHW preparation.

The central heating installation consists of steel pipes routed along the ceiling and surface-mounted on walls. The vertical connections to the radiators are partially installed in wall chases and partially exposed. There is either no thermal insulation or insulation with poor thermal properties. The system includes old cast-iron sectional radiators and some panel radiators. The radiators are designed for high-temperature heating systems. Weather-compensated control is implemented. Each radiator is equipped with thermostatic valves with thermostatic heads.

Domestic hot water is also prepared in the district heating substation. The pipes are surface-mounted, either uninsulated or fitted with thermal insulation that does not meet current standards for thermal resistance [27]. Current efficiency of DHW and CH systems is given in Table 2.

The building is powered solely by the municipal electricity grid, as is the case for about 90% of kindergartens located in the same urban area [29]. The source of both heat and electricity is the City Heat and Power (CHP) plant, which serves as the main energy provider for such facilities.

Figs. 5 and 6 present the thermal and electrical energy consumption in the kindergarten between 2022 and 2024. A seasonal reduction in thermal energy demand is observed each year from June to September, due to the lack of heating requirements during the summer months. In this period, thermal energy is used solely for heating DHW. A further reduction in one of the summer months (July or August) corresponds with the holiday break, when the kindergarten is closed to children and maintenance or cleaning operations take place. Electricity in the kindergarten was used for lighting and maintaining different equipment e.g. computers, washing machines, pumps.

Thermal energy consumption in the year 2022 amounted to 570.01 GJ, in 2023 to 495.20 GJ, and in 2024 to 498.10 GJ. When accounting for differences in standard seasonal conditions,required in energy audit calculations, these values provide a basis for evaluating energy efficiency improvements or changes in building operation. The annual consumption of active electrical energy for the years 2022–2024 was 12,772 kWh. 10,378 kWh. and 11,443 kWh, respectively.

Table 2
Current efficiency of DHW and CH systems [26].

Efficiency of:	DHW	CH
Generation	0.98	0.99
Distribution	0.50	0.96
Usage	1.00	0.77
accumulation	1.00	1.00
Total efficiency	**0.4900**	**0.7318**

5. Retrofitting scenarios

5.1. Development of retrofitting scenarios

The building currently demonstrates insufficient thermal insulation of its external elements and utilizes thermal and electrical energy derived from non-renewable sources. In response, 12 retrotiffing scenarios have been developed to reduce final energy demand for heating, DHW preparation, and electricity consumption from the power grid. These scenarios cover improvements in building envelope insulation (Scenarios 1–7), upgrades to the DHW installation (Scenario 8), refurbishment of the CH system (Scenario 9), and retrotiffing of energy supply systems (Scenarios 10a–10c).

The scenarios have been arranged according to the scale of intervention: – from the least extensive (Scenario 1) to the most comprehensive (Scenario 10c), – as presented in Table 3. Each subsequent scenario is an extension of the previous one, with the final Scenario encompassing all retrotiffing measures proposed. Individual interventions are ranked into variants based on their economic viability (defined by the SPBT index) based on a building energy audit [26]. The first variant contains the most cost-effective intervention (with the lowest SPBT), and projects with a longer payback period are added successively.

To ensure compliance with national thermal protection requirements in Poland, the retrofitting scenarios were selected so that the resulting U-values of upgraded components would reach levels below the recommended $U_{C,max}$ (Table 1). The sequence of interventions reflects a gradual improvement of the building envelope, beginning with simple upgrades and progress to more complex ones. These improvements include insulation of the entrance canopy (Scenario 1), external walls' insulation (Scenario 2), isolation of the flat roof (Scenario 3), replacing windows (Scenario 4) and doors (Scenario 5), insulating basement walls above ground (Scenario 6), and below ground (Scenario 7).

The resulting heat transfer coefficients (*U*-values) for each element of the building after implementing these thermal upgrades are listed in Table 4.

This approach ensures that all proposed interventions are both realistic and aligned with regulatory expectations for buildings located in the Cold Temperate Climate Zone.

In Scenario 8, an additional retrotiffing of the DHW system is proposed. This includes the replacement of pipes, the introduction of a circulation system equipped with thermostatic valves, and the thermal insulation of pipes from the heat source (district heating substation) to the points of use. All modifications are carried out in accordance with current regulations on the thermal resistance of DHW pipes [27]. These measures aim to improve the efficiency of the DHW system. The new DHW system efficiencies following retrotiffin were determined based on [18,19] and are presented in the Table 5.

The subsequent proposed solution – Scenario 9 – involves retrotiffing of the CH. It includes the replacement of piping and radiators, adapted to the reduced heat load of the rooms resulting from the thermal retrotiffing of the building envelope. The heat source in Scenario 9 remains the district heating substation, which continues to supply heat for both CH and DHW purposes. Pipe insulation will be implemented to reduce transmission losses, in accordance with current thermal resistance requirements [27]. The system will incorporate both central weather-compensated control (at the heat source) and local regulation via thermostatic radiator valves. The resulting efficiencies of the CH system after retrotiffing are summarized in Table 5.

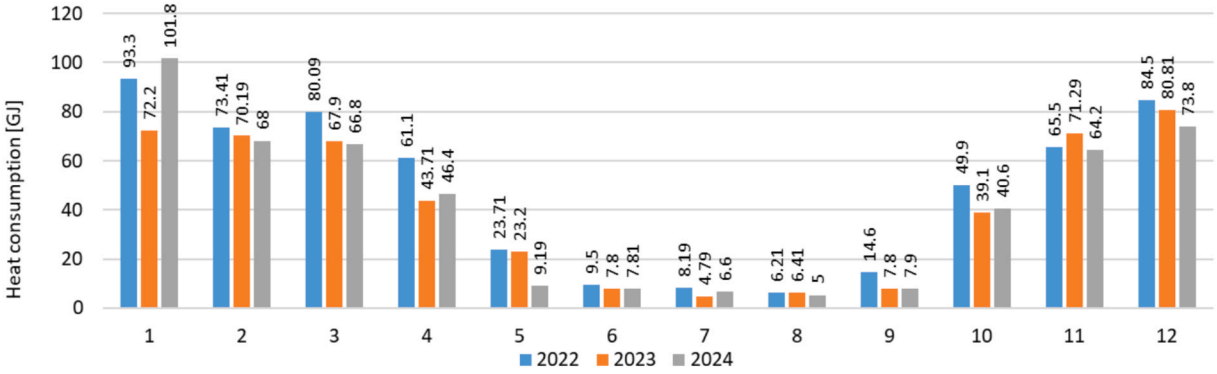

Fig. 5. Current heat consumption for purpose of CH and DHW systems in analyzed kindergarten in years 2022–2024 [Own elaboration based on invoices from ENEA Ciepło Sp. z o.o.].

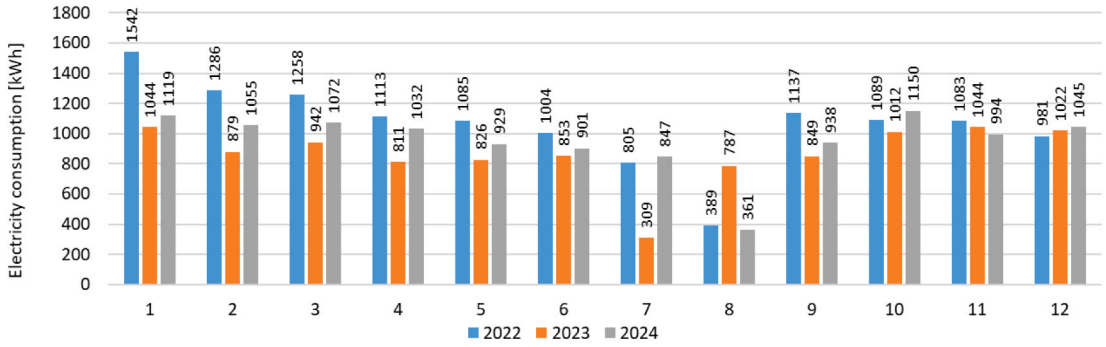

Fig. 6. Current electricity consumption in analyzed kindergarten in years 2022–2024 [Own elaboration based on data provided by PGE Dystrybucja].

Table 3
Interventions proposed in analyzed scenarios.

Intervention	Scenario											
	1	**2**	**3**	**4**	**5**	**6**	**7**	**8**	**9**	**10A**	**10B**	**10C**
Insulation of the canopy above the entrance vestibule	+	+	+	+	+	+	+	+	+	+	+	+
Insulation of external walls	–	+	+	+	+	+	+	+	+	+	+	+
Insulation of the flat roof	–	–	+	+	+	+	+	+	+	+	+	+
Replacement of windows	–	–	–	+	+	+	+	+	+	+	+	+
Replacement of doors	–	–	–	–	+	+	+	+	+	+	+	+
Insulation of basement walls (above ground)	–	–	–	–	–	+	+	+	+	+	+	+
Insulation of basement walls (below ground level)	–	–	–	–	–	–	+	+	+	+	+	+
Retrotiffing of DHW system	–	–	–	–	–	–	–	+	+	+	+	+
Retrotiffing of CH system	–	–	–	–	–	–	–	–	+	+	+	+
Replacement of the heat source	–	–	–	–	–	–	–	–	–	+	+	+
Replacement of the heat source + installation of PV panels	–	–	–	–	–	–	–	–	–	–	+	+
Replacement of the heat source + PV panels + energy storage system	–	–	–	–	–	–	–	–	–	–	–	+

Table 4
Heat transfer coefficients (U-values) for each element of the building after retrofitting [26].

Building element	***U* [W/m^{2}K]**
External walls	
– above-ground storeys	0.20
– basement walls above ground level	0.19
– basement walls below ground level	0.17
Roof / flat roof / ceiling under unheated attic or above open passageways	0.14
Windows and balcony doors	0.90
External doors and gates	1.30
Canopy over the entrance vestibule	0.29

Table 5
Efficiency of DHW and CH systems after retrotiffing.

Efficiency of:	DHW	CH
generation	0.98	0.99
distribution	0.60	0.96
Usage	1.00	0.88
accumulation	1.00	1.00
Total efficiency	**0.5880**	**0.8364**

The following three scenarios focus on the retrotiffing of the building's heat source and on-site electricity production, with the overarching goal of increasing independence level from the national power grid:

- Scenario 10A – Replacement of the existing district heating substation with an air-source heat pump.
- Scenario 10B – Installation of a new air-source heat pump in conjunction with a photovoltaic (PV) system, enabling partial on-site electricity generation.
- Scenario 10C – Implementation of a new air-source heat pump combined with both a PV system and an electricity storage system, enabling increased self-sufficiency and energy resilience.

Each scenario represents a stepwise approach to reducing the building's reliance on fossil fuels and the centralized energy infrastructure, with Scenario 10C offering the most comprehensive solution.

Scenario 10A involves the replacement of the existing district heating substation with a new air-source heat pump (ASHP) system. The primary motivation for this upgrade is to reduce the consumption of non-renewable primary energy and thereby lower the building's environmental impact. An air-to-water heat pump was selected due to site-specific constraints – namely, the extensive presence of mature trees surrounding the preschool facility. These conditions make the installation of ground-source heat exchangers technically challenging and ecologically undesirable, as it would necessitate extensive excavation and potential deforestation. The proposal is in line with Dai et al. [30] claims to use ASHPs as a heating method for the sustainability of residential buildings in clean space heating.

Scenario 10B builds upon the previous approach by incorporating PV panels to supply renewable electricity to the air-source heat pump. This configuration is designed to reduce the facility's reliance on the national power grid and further decrease carbon emissions associated with electricity consumption. Given the limited availability of unshaded land due to surrounding tree coverage, PV panels are proposed exclusively for rooftop installation.

Finally, Scenario 10C extends Scenario 10B by adding an electrical energy storage system. As suggested by Santecchia et al. [31] overcoming the challenge posed by the inherent variability of renewables can be accomplished by either overbuilding generation resources or prioritizing electricity storage. The primary objective of the battery integration is to balance the temporal mismatch between solar energy generation and building energy demand. Without storage, a significant portion of PV-generated electricity may be exported to the grid or wasted. By smoothing out the variability inherent in renewable energy production, the storage system enhances energy autonomy and operational resilience of the preschool facility. Battery systems allow excess electricity generated by the PV array during peak sunlight hours to be stored and used later, – particularly in the early morning, evening, or during cloudy periods, – when solar generation is minimal. This minimizes reliance on grid-supplied electricity during peak tariff hours and contributes to load balancing. Summarizing, Scenario 10C enables higher self-consumption rates, improving the return on investment of the PV system and maximizing the environmental benefit of installed renewables.

What is more, preschool, as public educational facility could serve as a model of sustainable infrastructure, demonstrating to students and their parents the practical integration of renewable energy, smart grids, and energy storage technologies. Thus, such solutions should be supported by local governments.

5.2. Retrofit of the heat source

For the analyzed preschool building, a cascade system including two air-to-water heat pumps operating in parallel was selected, in accordance with manufacturer recommendations [32]. The chosen model is specifically designed for retrofitted buildings with existing central heating systems with panel radiators. These heat pumps could operate efficiently under very low outdoor temperatures, down to –22°C. and are able to deliver supply water temperature up to 65°C. This high-performance capability allows for monoenergetic operation, meaning that the heat pumps alone can meet nearly the entire heating demand without auxiliary heating sources under most wheather conditions.

For a calculated heating demand of 80 kW, the two-pump cascade system can cover 99.9% of the annual heating energy requirement. The system's bivalence point, the outdoor temperature below which auxiliary heating becomes necessary, is at –19°C. Below this threshold, heating will be supplemented by an electric immersion heater, which is the part of the heat pump. However, due to climate change and evolving weather patterns, design temperatures for kindergarten location (–22°C) nowadays occur very infrequently, making the need for auxiliary heating source increasingly rare.

The performance parameters of a single air-to-water heat pump unit, as specified in the manufacturer's catalogue [32], are as follows:

- Nominal heating capacity at A–7/W35 (per EN 14511): 47.90 kW
- Coefficient of performance (COP) at A–7/W35 (per EN 14511): 3.60
- Maximum outlet temperature of the heating medium: 65°C
- Operating range of the heat source (ambient air): –22°C to + 40°C [32].

Based on the manufacturer's data, a functional approximation was developed to describe the relationship between the Coefficient of Performance (COP) and the outdoor air temperature T_{out} for the heat pump. This relationship is expressed [32] by the empirical formula (4) and presented in Fig. 7:

$$COP = 0.152\ T_{out} + 3.650 \quad (4).$$

The function approximating the heat pump's heating output $P(t_{out})$ is defined [32] by the relation (5) (Fig. 7):

$$P = 2.340\ T_{out} + 111.40 \quad (5).$$

To estimate the energy demand for domestic hot water preparation, it was assumed that hot water consumption occurs between 6:00 and 17:00, corresponding to the operating hours of the kindergarten.

5.3. Retrofit of the electricity source

Due to the requirement for higher efficiency under suboptimal solar lighting conditions and the relatively longer lifespan compared to other commercial technologies, modern monocrystalline TOPCon PV modules based on PERC cells were selected. These modules feature an advanced structure incorporating a thin tunnel oxide layer and a polycrystalline silicon passivation layer. Specifically, the Tiger Neo 480 Wp N-Type Mono panels with a peak power output of 480 Wp were chosen [33]. The high-power rating of each individual panel reduces the total number of components required in the PV system. Each panel has dimensions of 1903 × 1134 × 30 mm, translating to an approximate area requirement of 3.3 m^2 per module, including spacing.

Due to the kindergarten's location and the high density of surrounding trees, the roof was identified as the most suitable site for PV installation. The total roof area is 445 m2, with a technical safety margin of 25% applied to account for access paths, structural limitations, and obstructions. This results in a net available roof area of approximately 334 m2. An inter-row spacing of ~ 1.1 m was incorporated based on a 35° tilt angle, ensuring minimal shading between panel rows. Additionally, to avoid overengineering the system and to maintain a balanced match between PV generation and the building's transitional-season electricity demand, while also considering the planned installation of a battery storage system, the PV system was limited to 50 modules, that corresponds to a total installed peak power of 24 kWp.

For the analyzed 24 kWp PV system, an energy storage system was considered in scenario 10C to increase self-consumption and enable the storage of daytime energy surpluses. The proposed storage capacity corresponds to approximately 150% of the average daily electricity generation. Based on performance estimates, the average daily energy production of the PV system is approximately 55.9 kWh/day. Accordingly, the target usable storage capacity was set at around 80 kWh. To meet this requirement, a lithium iron phosphate ($LiFePO_4$) battery

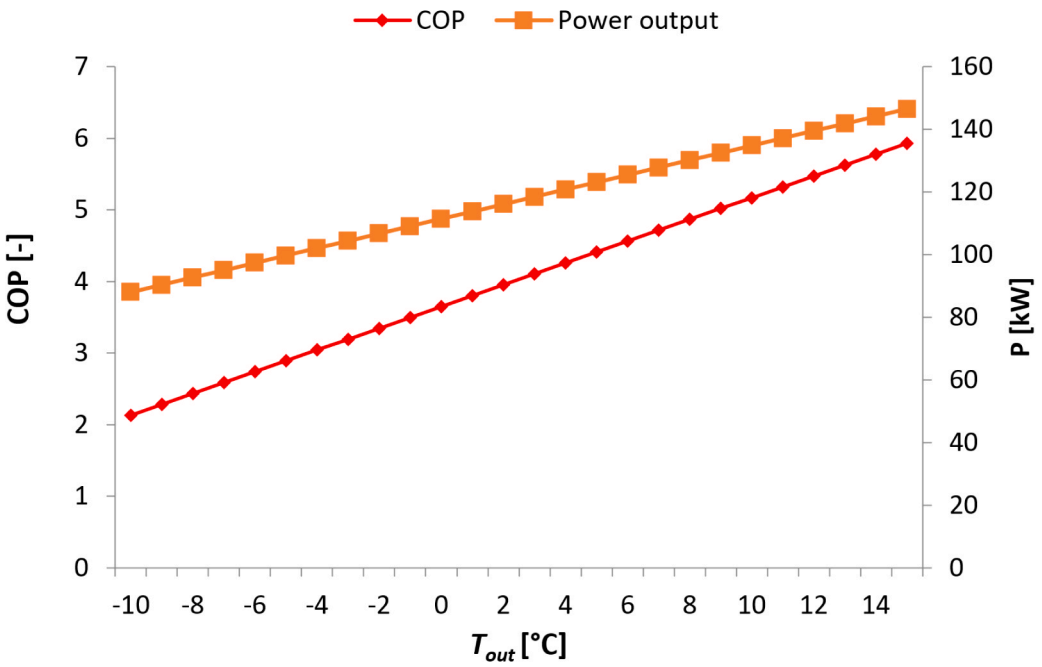

Fig. 7. Relation between the COP, the power output and the outdoor air temperature T_{out} for the analyzed heat pump.

system with a total capacity of 100 kWh was selected [34,35]. This system will allow for the accumulation of excess solar energy generated during the day, which can be utilized later during periods of low or no generation (e.g., evening, night, or overcast days).

To assess the performance of this configuration, a simulation model was developed to analyze the interaction between the PV system and the battery storage, accounting for energy production profiles, consumption patterns, and charging/discharging behavior.

In order to reflect the actual operation of the PV system in conjunction with the energy storage and the power grid, the following assumptions were made in the simulation model:

- Priority of PV Usage: Electricity generated by the PV system is primarily used to power the air-source heat pump, provided that there is a concurrent electricity demand from the pump.
- Energy Surplus Management: Any excess electricity not used by the heat pump is directed to charge the battery. If the battery reaches its maximum state of charge, the remaining surplus is exported to the national power grid.
- Electricity Demand Coverage Hierarchy: The building's electricity demand is met in the following order of priority:
- (1) Direct supply from the PV system,
- (2) Discharge from the battery storage,
- (3) Import from the grid, only when the above two sources are unavailable.
- Round-Trip Efficiency: The average round-trip efficiency of the lithium iron phosphate ($LiFePO_4$) battery is assumed to be 95%.
- Battery Operating Range: Maximum state of charge assumed as 90 kWh while minimum state of charge at the level of 20 kWh.

These operational assumptions were implemented in the simulation to evaluate system performance under realistic operating conditions and control strategies.

Two key energy performance indicators for the PV system are estimated as follows:

- Self-consumption ratio SCR (6), defined as the share of PV-generated electricity that is directly consumed on-site, informs what percentage of the energy produced from the PV system was consumed on site:

SCR = electricity directly utilized from the PV system and possibly supported by an energy storage / total PV generation [%] (6).

- Self-sufficiency ratio SSR (7), defined as the share of total electricity demand that is covered by the PV system and energy storage if present, informs what percentage of the total energy consumption in a given location was covered by PV energy (possibly supported by an energy storage):

SSR = electricity directly utilized from the PV possibly supported by an energy storage / total energy demand (7).

6. Environmental life cycle assessment (LCA)

6.1. Scope of the study

The life cycle assessment (LCA) involves the definition of the functional unit and system boundaries and subsequently excluding products irrelevant to the study.

According to the international LCA standards ISO 14040/44 [23,24], the functional unit (FU) is defined as "a quantified performance of a product system for use as a reference unit". In this case, determining the functional unit was particularly challenging due to the use of multiple insulation materials, construction elements, and thermal retrotiffing devices. A declared unit was adopted, which relates the product's material flows to its environmental impact. For this study, the functional unit was defined as the total scope of thermal retrotiffing necessary to achieve the assumed energy goals.

The system boundaries encompassed all life cycle stages – i.e., cradle-to-grave.

The first phase focuses on the product manufacturing process in each thermal modernisation option. The analysis includes raw material supply (environmental impacts resulting from the extraction of new materials and resources or the reuse of materials and resources); raw material

transport (includes emissions generated during transport from the extraction site to the production plant); production stage (consists of production processes, including the production of ancillary products and components, as well as assembly and transformation processes to obtain the final product).

The transportation phase (A4) of finished products to the construction site was also omitted to high data uncertainty. Additionally, many publications on life cycle analyses in construction have shown a small share of the transport phase in total CO_2 emissions [36,37,38]. The construction phase (A5) was also considered insignificant from the point of view of environmental impact over the entire 30-year life cycle [36,37,38]. The construction phase (A5) was also considered insignificant from the point of view of environmental impact over the entire 30-year life cycle.

For Scenarios 1–9, the use phase was excluded as non-relevant. Scenarios 10A-10C, on the other hand, include the B4-Replacement and B5-Refurbishment phases, as it is assumed that equipment will need to be replaced during the 30-year life cycle. Scenarios 10A-10C also analyse energy inputs from non-renewable sources during operational energy consumption. Energy from the grid is not included here. CO_2 emissions from this process were calculated based on Poland's energy mix, using real-world data on fuel combustion in combined heat and power plants.

In addition, the environmental impacts arising from the processing of materials, components, and devices at the end of their service life were considered (e.g., hazardous waste disposal, thermal waste disposal, recycling of PV panels, etc.). Where data availability in the Sphera database [39] allowed, End-of-life stages were included. For options 10A–10C, environmental benefits from using energy from renewable sources were additionally considered. In options 1–9, there are no environmental benefits. The life cycle stages covered in the collected EPDs are summarized in Table 6.

The life cycle of the investment was set at 30 years. Within this period, no replacement or retrotiffing is planned for the thermal insulation of building elements (Scenarios 1–7), hot water installation (Scenario 8), and central heating installation (Scenario 9). In the case of equipment replacement (Scenario 10A, 10B and 10C), the service life period of 15 years is assumed for the installed devices (e.g., heat pumps, photovoltaic systems, batteries). Consequently, a single replacement of these components is expected to occur once within the 30-year assessment period.

This time horizon ensures a comprehensive evaluation of both operational performance and long-term environmental impact in the Life Cycle Assessment.

6.2. Life cycle Inventory (LCI)

The Life Cycle Inventory (LCI) phase includes a quantitative account of all energy, material and emission flows associated with the system covered by this study throughout its life cycle. The first phase focuses on the product manufacturing process in each thermal modernisation option. The analysis includes raw material supply (environmental impacts resulting from the extraction of new materials and resources or the reuse of materials and resources); raw material transport (includes emissions generated during transport from the extraction site to the production plant); production stage (consists of production processes, including the production of ancillary products and components, as well as assembly and transformation processes to obtain the final product). Scenarios 10A-10C also analyzse energy inputs from non-renewable sources during operational energy consumption. Energy from the grid is not included here, CO_2 emissions from this process were calculated according to the energy mix used in Poland. In addition, the environmental impacts occurring during the processing of materials, components and devices at the end of their service life were considered (e.g., disposal of hazardous waste. thermal waste disposal, recycling of PV panels, etc.).

The assumptions for each analyzed scenario are summarized in ANNEX B. The primary data sources included information obtained from technical documentation regarding the thermal retrotiffing of the building envelope, documentation of designed systems (like central heating and DHW) and manufacturers datasheets for all elements included in each retrotiffingscenario:

- Data on thermal insulation methods [41]
- Data on windows and doors replacement [42]
- Data on CH and DHW retrotiffing: pipes [43], radiators [44], valves [45]
- Data on heat pumps [32].

A literature review was conducted to supplement missing or uncertain data, particularly in relation to the performance and environmental parameters of:

- Heat pumps (e.g., efficiency, refrigerant type, service life) [45-47]
- Photovoltaic panels (e.g., material composition) [48,49,50]
- Energy storage systems (e.g., capacity degradation, round-trip efficiency, material composition) [51].

This integrated data approach ensures a more robust and comprehensive basis for the subsequent Life Cycle Assessment (LCA).

Table 6
Life cycle included in the analysis [40].

Life Cycle Stages			Scenarios											
			1	2	3	4	5	6	7	8	9	10A	10B	10C
Product stage	Raw material supply	A1	X	X	X	X	X	X	X	X	X	X	X	X
	Transport	A2	X	X	X	X	X	X	X	X	X	X	X	X
	Manufacturing	A3	X	X	X	X	X	X	X	X	X	X	X	X
Construction process stage	Transport	A4												
	Construction	A5												
Use stage	Use	B1												
	Maintenance	B2												
	Repair	B3												
	Replacement	B4										X	X	X
	Refurbishment	B5										X	X	X
	Operational energy use	B6										CO_2 emissions calculated baseline on Polish energy mix (Table 9)		
	Operational water use	B7												
End-of-life stage	Deconstruction/ Demolition	C1												
	Transport	C2												
	Waste processing	C3	X	X	X	X	X	X	X	X	X	X	X	X
	Disposal	C4	X	X	X	X	X	X	X	X	X	X	X	X
Benefits and loads beyond the system boundaries	Reuse – Recovery – Recycling potential	D										X	X	X

The operational CO_2 emissions from combustion in fuels in the current state of the building and after the retrofit were determined as the product of the final energy demand and the emission factor for the fuel. For the municipal heating network supplying heat both for CH ~~central heating~~ and for the DHW preparation ~~of domestic hot water~~, the emission factor was determined based on the data from the heat producer [52] and data for fuels [53] ~~and~~. It amounted to 52.229 kg/GJ. For electricity emission factor amounted to 52.229 kg/GJ. For electricity consumption at the end-user level, an emission factor of 597 kg CO_2 per MWh was applied, based on data from [53].

7. Results

7.1. Energy demand for the building

Each of the nine scenarios related to the retrotiffing of the building envelope and the central heating (CH) and domestic hot water (DHW) systems was analyzed in terms of its impact on reducing the thermal energy demand for space heating, ventilation, and hot water preparation (HVAC). The results of the analysis ~~based on~~ [26], are presented in Table 7, which summarizes both useful and final energy demand for each retrofit scenario.

Scenarios 1 through 7, which address the thermal insulation performance of the building envelope, demonstrate a progressive reduction in both useful and final energy demand for space heating and ventilation. In contrast, the energy demand for domestic hot water (DHW) remains constant across all scenarios, as thermal insulation improvements do not affect DHW system performance. Scenario 1, involving only canopy insulation, led to the smallest reduction in final energy demand – just 0.18% compared to the baseline. Scenario 2, which adds external wall insulation to the canopy upgrade, yields a significant reduction of nearly 29% in total final energy demand. The following scenario (Scenario 3) includes the addition of flat roof insulation and it further reduces final energy consumption by approximately 39% compared to the current state and by about 35% relative to Scenario 2. This highlights the critical role of roof heat losses in the building's overall energy balance. Scenario 4, which includes window replacement, results in a total reduction of 51.6%, representing a 32% decrease compared to Scenario 3. In Scenario 5, the replacement of exterior doors contributes a relatively minor improvement – a further 2% reduction compared to Scenario 4 and a total savings of 52.6% relative to the original condition. Scenario 6, which includes insulation of above-ground basement walls, achieves an additional 5% reduction in final energy demand compared to Scenario 5 (55% relative to the baseline). Finally, Scenario 7, which proposed additional insulation of below-ground basement walls, leads to an additional 9% reduction, culminating in a total final energy savings of approximately 60% for space heating, ventilation, and DHW compared to the current state.

The subsequent retrofit scenarios (8–10C) involve upgrades to domestic hot water (DHW) and central heating (CH) systems. As these changes do not affect the building envelope, the useful energy demand remains unchanged. However, there is a significant impact on the total final energy demand due to increased system efficiencies.

Retrotiffing of the DHW system in Scenario 8 led to a 16.7% reduction in final energy demand for hot water preparation. This corresponds to an overall reduction of approximately 62% in final energy demand for space heating, ventilation, and DHW compared to the current (baseline) state. The addition of CH system retrotiffing (Scenario 9) results in a total final energy savings of around 66% compared to the baseline and an additional 6% reduction relative to Scenario 8.

The calculated heating load of the building prior to retrotiffing was 124.82 kW. Following the implementation of thermal insulation measures and CH system upgrades. the heating load was reduced to 79.97 kW, representing a 44% decrease. This reduction in design heating demand enables the downsizing of CH system components, including radiators, piping, and control valves. Furthermore, it allows for a lower supply temperature of the heating medium, which is particularly advantageous when transitioning to low-temperature heat sources such as air-source heat pumps.

The last analyzed scenarios included the change of heat source end electricity source. The results of useful and final energy demand for these scenarios (10A-10C) are presented in Table 8.

Upgrading the heat generation system by introducing a high-efficiency air-source heat pump (Scenario 10A) contributes to a substantial 91% reduction in total final energy demand compared to the current state, heat pump's high seasonal performance factor (SPF) and a 39% reduction relative to Scenario 9. This dramatic decrease is primarily due to the high seasonal performance factor (SPF) of the heat pump, calculated at 2.74, which significantly reduces the input energy required for heating purposes.

The final energy values for domestic hot water (DHW) and space heating (CH) in Scenarios 10A–10C are not simple sums of the individual end-use energy demands. This is because the system operation model incorporates a DHW priority logic, which affects the allocation of energy use between the two functions. In this context, the final energy values for DHW and CH are not derived by dividing the useful energy values (from the reference tables) by the system efficiency. Instead, they are the result of detailed hourly simulations conducted using the methodology proposed by Werner-Juszczuk and Krawczyk [29], which calculates the system's energy behaviour for each hour of the year. The reported final energy for Scenarios 10A–10C refers exclusively to the electricity drawn from the power grid that is required to operate the air-source heat pump, specifically the compressor of the thermodynamic cycle. Importantly, these values do not represent the total heat demand of the building adjusted for system efficiency, as the adopted methodology does not account for the thermal energy extracted from the heat pump's low-temperature source – in this case, ambient air. Therefore, the final energy values should be interpreted as the external electricity input, not

Table 7
Useful and final energy demand for the analyzed retrofitting scenarios.

Scenario	Useful energy demand for space heating $Q_{H,nd}$ [GJ]	Heating system efficiency [-]	Final energy demand for space heating [GJ]	Useful energy demand for DHW Q_w [GJ]	DHW efficiency [-]	Final energy demand for DHW [GJ]	Final energy demand in total [GJ]	Annual energy savings [GJ]	[%]
actually	559.48	0.7318	764.53	35.07	0.4900	71.57	836.10	–	–
1	558.41	0.7318	763.06	35.07	0.4900	71.57	834.63	1.47	0.18
2	382.51	0.7318	522.7	35.07	0.4900	71.57	594.27	241.83	28.92
3	319.97	0.7318	437.24	35.07	0.4900	71.57	508.81	327.29	39.14
4	243.64	0.7318	332.93	35.07	0.4900	71.57	404.50	431.60	51.62
5	237.97	0.7318	325.18	35.07	0.4900	71.57	396.75	439.35	52.55
6	222.27	0.7318	303.73	35.07	0.4900	71.57	375.30	460.80	55.11
7	190.46	0.7318	260.26	35.07	0.4900	71.57	331.83	504.27	60.31
8	190.46	0.7318	260.26	35.07	0.5880	59.64	319.90	516.20	61.74
9	190.46	0.8364	227.71	35.07	0.5880	59.64	287.35	548.75	65.63

Table 8
Energy savings in scenarios connected with the energy source replacement.

Scenario	Useful energy demand for space heating $Q_{H,nd}$ [GJ]	Heating system efficiency [-]	Final energy demand for space heating [GJ]	Useful energy demand for DHW Q_w [GJ]	DHW efficiency [-]	Final energy demand for DHW [GJ]	Final energy demand in total [GJ]	Annual energy savings [GJ]	[%]
10A	190.46	2.34	67.80	35.07	1.6400	35.43	71.95	764.15	91.40
10B	190.46	2.34	67.80	35.07	1.6400	35.43	56.12	779.98	93.29
10C	190.46	2.34	67.80	35.07	1.6400	35.43	45.93	790.17	94.51

the total thermal output delivered to the building.

The simulation of heat pump performance for Scenario 10A enabled the determination of electricity consumption by the cascade of air-source heat pumps for both space heating (CH) and domestic hot water (DHW). The hourly thermal energy demand for each hour of a typical meteorological year was used as input and is illustrated in Fig. 8. The total annual electricity consumption of the heat pump system for both CH and DHW purposes was calculated to be 19,985 kWh, based on a Seasonal Coefficient of Performance (SCOP) of 2.74.

This SCOP value reflects both the high required supply temperature of the heating medium in the building's CH system (due to radiator-based heat distribution) and low outdoor air temperatures during a long part of the heating season.

In Scenario 10B, it is proposed to install an air-source heat pump supported by an on-site photovoltaic (PV) system. As described in Section 4.2, the recommended PV system has a peak power output of 24.0 kWp. Based on data from the Photovoltaic Geographical Information System (PVGIS) [54], the expected annual electricity generation from this system is 20,417.9 kWh/year (see Fig. 9).

In Scenario 10B, the electricity directly utilized from the PV system for building operation amounts to 4,396.9 kWh/year, out of a total PV generation of 20,417.9 kWh/year.

The electricity drawn from the national grid is 15,587.8 kWh/year, while the surplus PV electricity exported to the grid reaches 16,021.1 kWh/year. Two key energy performance indicators for the PV system: SCR and SSR, estimated using Equation 5 and 6, are equal to 23.3% and 22.0% respectively.

These values indicate that while the PV system significantly contributes to local generation, the limited overlap between PV production and building demand – particularly for heating – restricts direct self-consumption, justifying the consideration of energy storage (as in Scenario 10C). The simulation results are presented graphically in Fig. 10.

In the analysis of the relationship between the demand for electricity and the availability of solar radiation for the analyzed facility, a clear discrepancy is visible (Fig.11). The greatest demand for energy falls in the winter months, when solar radiation reaches its minimum values. In the summer, despite the high availability of solar energy, the consumption of electricity decreases. This inversely proportional relationship poses a significant challenge for the effective balancing of local renewable sources, especially photovoltaics. This means that the potential for energy production from PV installations is greatest when the demand is the lowest – and vice versa. This necessitates the use of energy storage, as presented in Scenario 10a, and flexible demand management or integration with other sources to ensure system stability.

In the case of location, like the one under investigation, with relatively high climatic seasonality these differences are particularly visible and may affect the design of the local energy strategy.

In Scenario 10C, an extension of the PV system is proposed by incorporating an energy storage system with a capacity of 100 kWh. In this scenario, the amount of electricity directly utilized from PV generation remains the same as in Scenario 10B, namely 4,396.9 kWh/year. However, when accounting for the operation of the battery energy storage system and considering a 95% round-trip efficiency, the total utilization of electricity generated by the PV system increases by 2,829.2 kWh/year, reaching a total of 7,226.1 kWh/year. Electricity imported from the power grid amounts to 12,758.6 kWh/year, while electricity exported to the grid reaches 12,895.9 kWh/year. The self-consumption ratio is 38.3%, and the system's self-sufficiency is 36.2%.

A clear improvement in PV system performance can be observed with the integration of the battery storage, particularly during the transitional seasons. In summer, the battery reaches full charge due to excess generation, and surplus electricity is fed into the grid. The high state of charge during this period is clearly visible in Fig. 12, which illustrates the battery charging profile. This behaviour results from significantly reduced electricity demand during the summer months.

In contrast, during winter, electricity demand rises – primarily due to the increased operation of the heat pump with high energy demand for heating – while available solar irradiation decreases considerably. This leads to a visibly lower battery State of Charge (SoC). The resulting energy deficit is covered by electricity drawn from the power grid.

7.2. LCA results

Initially, each suggested thermal retrotiffing option's CO_2 emissions were examined. Fig. 13 displays the individual interventions' life-cycle

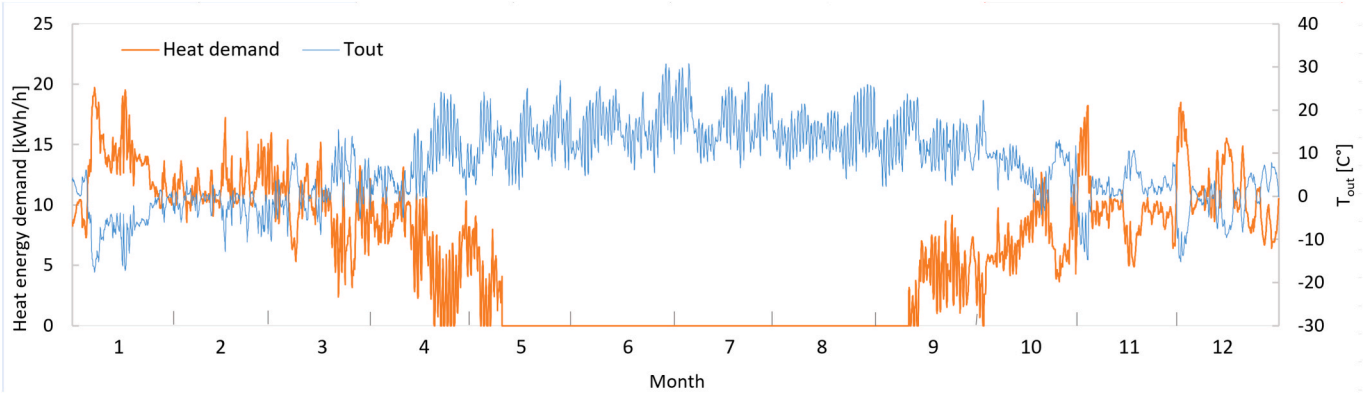

Fig. 8. Heat energy demand for central heating system of the building and outdoor temperature T_{out} in each hour of typical year.

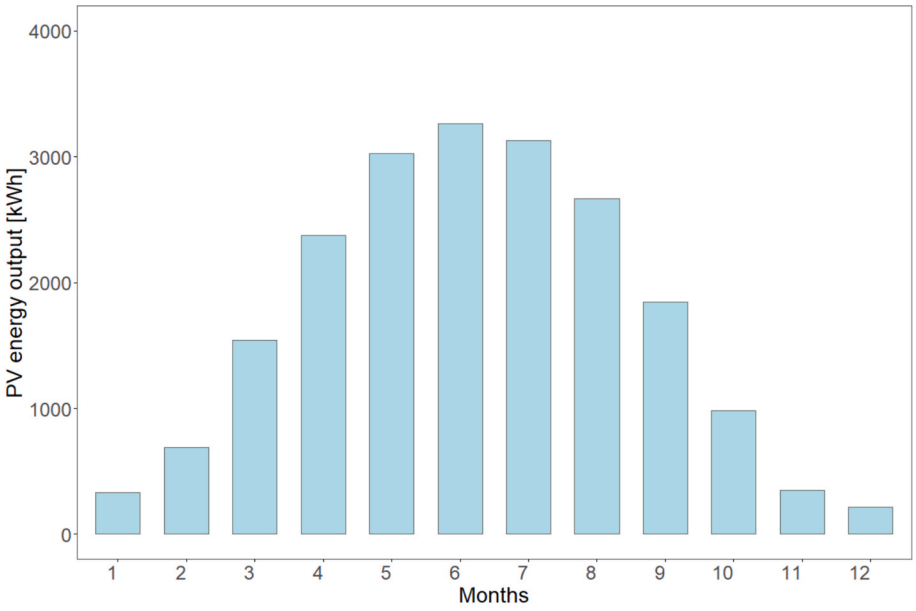

Fig. 9. Annual electricity generation from PV system [54].

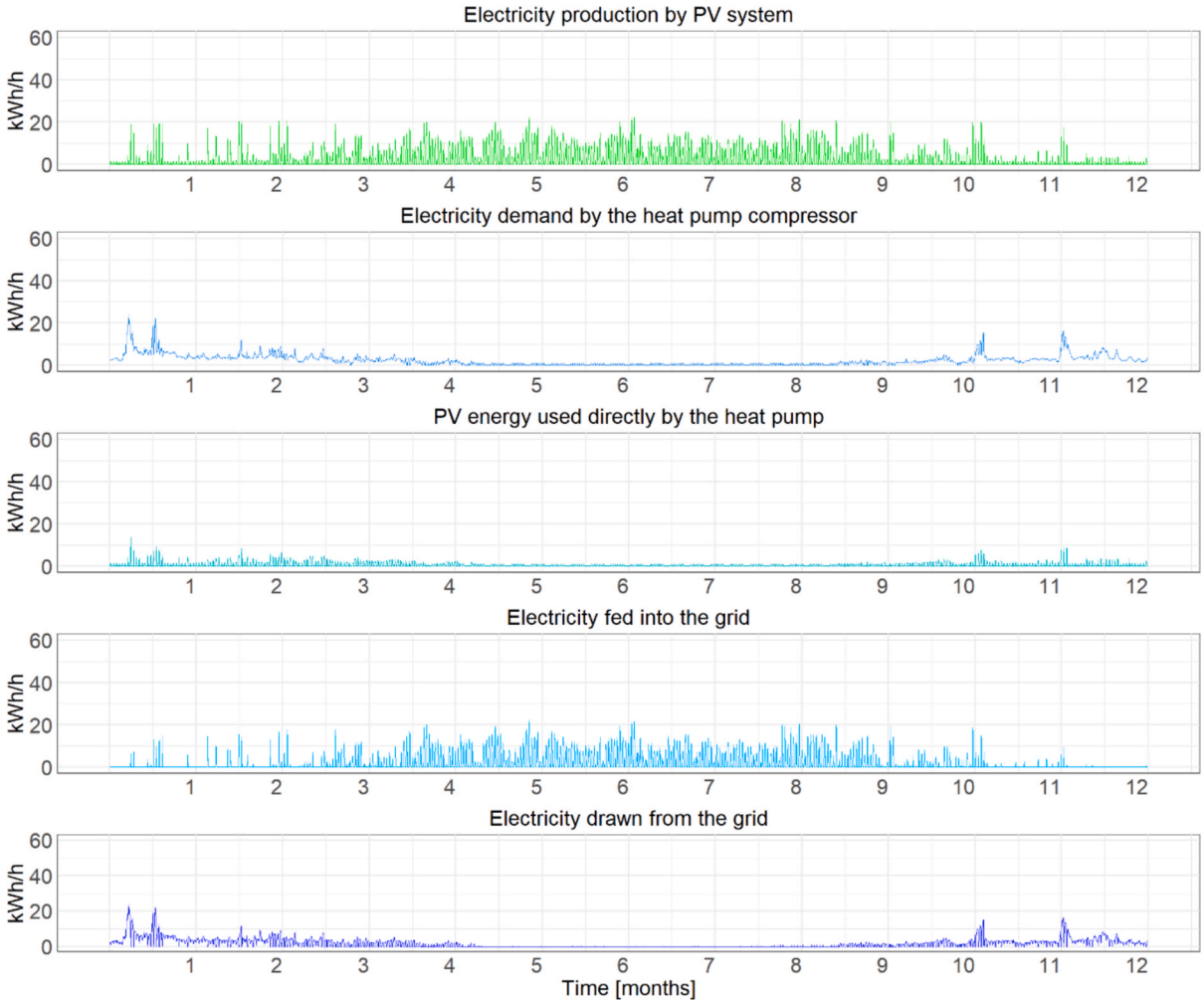

Fig. 10. The shares of individual systems in the processes of electricity generation, consumption, and the amount of energy fed into and drawn from the power grid in Scenario 10B.

CO_2 emissions.

The intervention involving the replacement of the heat source, 10A,

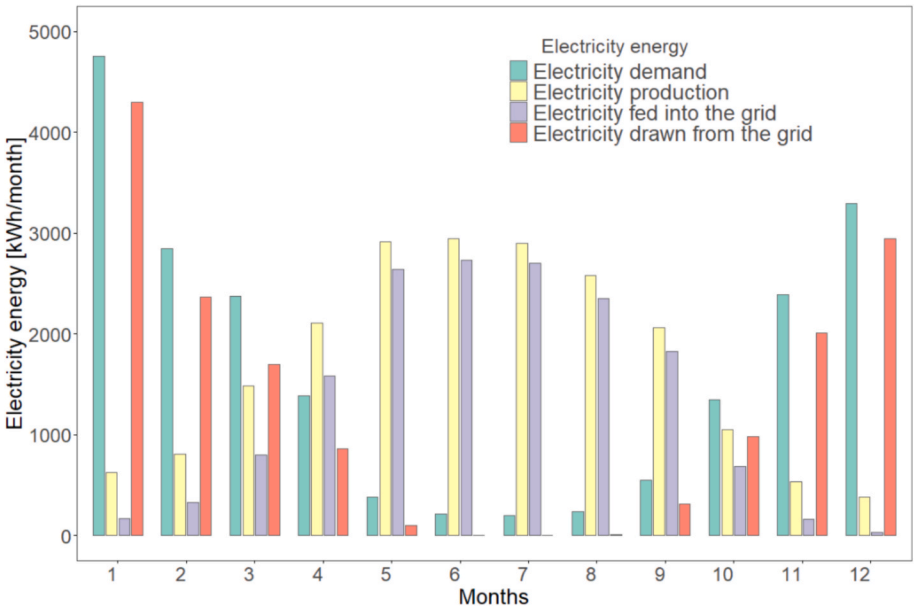

Fig. 11. Share of individual systems in electricity generation processes, its consumption and the amount of energy fed into the grid and taken from it in scenario 10B for individual months during the year.

shows negative life-cycle CO_2 emissions. This outcome is attributed to the environmental credit granted for electricity derived from renewable energy sources (*credit for electricity from renewable sources*). The use of a heat pump, powered by renewable electricity, significantly reduces the system's carbon footprint by displacing emissions that would otherwise result from conventional fossil-fuel-based heating systems.

Similar environmental benefits are also evident in the interventions that combine heat source replacement with photovoltaic (PV) installations and battery energy storage. In these configurations, the use of electricity generated by the PV system further offsets emissions by reducing the dependence on grid electricity. The battery storage enhances this effect by increasing on-site consumption of renewable energy, particularly in periods of high solar generation and low demand. As a result, these combined interventions not only improve energy autonomy but also lead to substantially lower or even negative net CO_2 emissions over the system's life cycle.

Environmental credits come not only from the use of renewable energy but also from the inclusion of phase D in the life-cycle analysis. According to the LCA for Expert, the recycling rate for large equipment such as pumps, boilers, and energy storage systems is 85–95%. This has also led to an increase in the value of environmental benefits.

These findings underline the importance of integrating renewable generation and storage technologies in building energy systems, particularly when evaluated from a life-cycle perspective.

Analysis of CO_2 emissions in scenarios, each of which is an extension of an earlier intervention, was the next stage. Fig. 14 shows CO_2 emissions in all scenarios over a 30-year life cycle. Scenario 10A's CO_2 emissions are substantially less than Scenario 9′s due to the introduction of a heat pump.

Operational CO_2 emissions (related to energy used for space heating and hot water preparation) over the 30-year period of use of the building were determined using the method described in 5.2, and the results are presented in Table 9.

In the individual scenarios, CO_2 emissions related to maintenance are decreasing, which is the result of reduced energy demand due to retrotiffing interventions. In scenarios 1–9, the percentage reduction in operational emissions is equal to the percentage reduction in heat demand, presented in Table 8, and is as much as 65.63%. Further reduction in operational emissions is possible by replacing heat sources with RES.

8. Discussion

8.1. CO_2 emissions

The results demonstrate that operational CO_2 emissions dominate across all retrofit scenarios, while embodied emissions account for a considerably smaller share—ranging from 0.01% in Scenario 1 to 17.63% in Scenario 10C (Table 9).

This relatively low share of embodied CO_2 emissions reflects the nature of retrofitting, in which only selected elements of the existing building are replaced, while the majority of the existing envelope and system remain unchanged. To enable a more transparent comparison of scenarios, the CO_2 emissions were normalized per unit of final energy saved over a 30-year period (Table 10). Due to the dominant share of operational CO_2 emissions in the total CO_2 emissions during retrofitting, the amount of reduced kg of CO_2 is close to the unit emission of the fuel consumed in the building.

Therefore, an additional indicator associated with the implementation of individual interventions was determined (Fig. 15). For this purpose, life-cycle carbon dioxide emissions for individual interventions, both excluding and including operational CO_2 emissions, were divided by the amount of final energy saved over a 30-year life cycle..

Given that operational emissions constitute the largest portion of life-cycle impacts, the CO_2 emission rate per GJ saved is closely aligned with the emissivity of the fuel used in the baseline condition. Among construction-oriented measures (Scenarios 1–9), the greatest absolute CO_2 reductions are achieved by external wall insulation, window replacement, and flat roof insulation, each exceeding 100,000 kg CO_2 in savings (Scenarions 2–9). However, when emissions are expressed per GJ saved, several envelope measures exhibit higher carbon intensities due to the embodied impacts of materials (range 49.39–50.5%), highlighting the importance of assessing both operational and embodied components simultaneously.

8.2. Introduction of new indicator

To compare the CO_2 reduction efficiency of individual retrotiffingprojects for the individual intervention scenarios, a new CO_2 reduction efficiency indicator – RCO_2 was proposed. The proposed indicator is intended to bridge the gap between energy and emissions. The

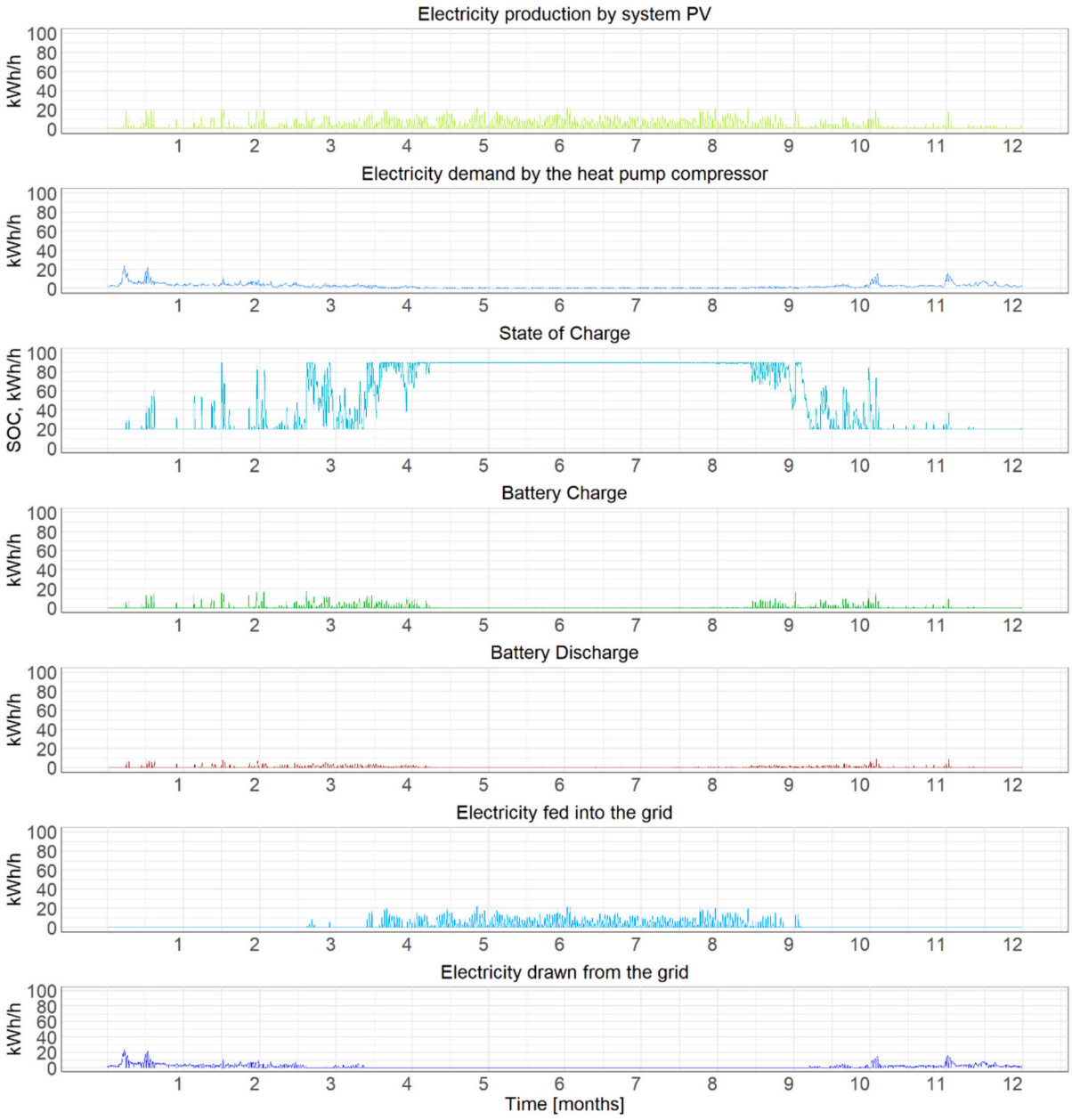

Fig. 12. Shares of individual subsystems in electricity generation and consumption, battery charging and discharging levels, and the amount of energy imported from and exported to the power grid. as well as the battery charging profile in Scenario 10C.

indicator is expressed according to the following relationship (8):

$$RCO_2 = \frac{\Delta CO_2}{\Delta E} \times \frac{1}{A} \quad (8)$$

where: ΔCO_2 represents the CO_2 emission reduction [kg/year], ΔE represents the energy consumption reduction [kWh/ year), and A is usable building area [m^2].

Defined as the ratio of annual CO_2 reduction to energy savings per unit of usable floor area, RCO_2 allows for normalized comparisons across buildings regardless of scale or cost. Higher RCO_2 values indicate greater climate efficiency.

The RCO_2 values for the analyzed kindergarten are presented in Fig. 13. According to the adopted methodology required by the Polish legislator, the greatest emission reduction efficiency is achieved by using an energy storage system, with an RCO_2 value of 0.075 $kgCO_2$/(kWh·m^2·year). This solution contributes 25% to the total reduction. The next two most effective measures are modernizing the heating system and replacing windows, with RCO_2 values of 0.057 and 0.038 $kgCO_2$/(kWh·m^2·year), respectively.

Moreover, the RCO_2 indicator is not affected by systemic climate variations for constant energy mix. In fact, energy savings in these conditions impact both CO_2 emission reduction and energy consumption reduction equally. In countries where the decarbonization policy could modify the energy mix, changes in this indicator may occur, but this comparison is out of the main scope of the present paper.

The relationship between annual energy savings and CO_2 emission rates presented in Tables 7-10 is clear. The higher the annual energy savings after renovation, the lower the CO_2 emissions. However, as can be observed, this relationship does not relates to the values of the proposed RCO2 indicator presented in Fig. 13. The RCO_2 indicator value does not demonstrate either a direct or inverse relationship with the emission values and annual savings. For scenarios 1 to 4 RCO_2 increases, then a decrease is observed for scenarios 5 and 6, after which it increases again for scenario 7. Even larger fluctuations are observed for scenarios

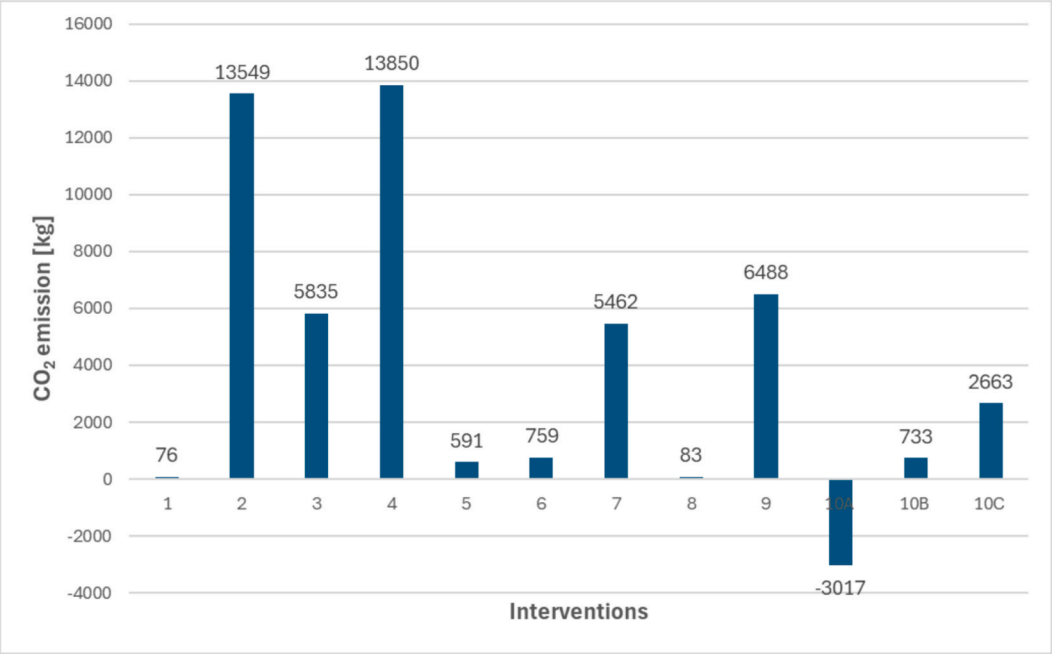

Fig. 13. Comparison of life-cycle carbon dioxide (CO_2) emissions for the individual intervention scenarios [kg].

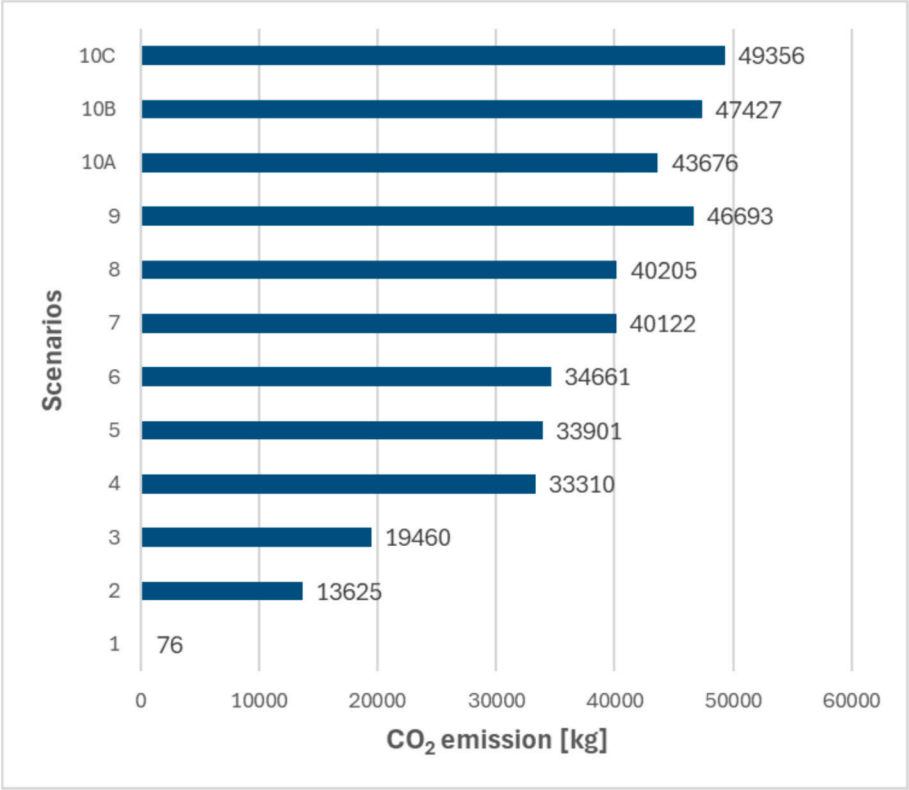

Fig. 14. CO_2 emission in all scenarios during 30-year life cycle.

from 8 to 10c. This results from the definition of the proposed indicator (formula ~~87~~). As can be observed, the ratio of CO_2 emission reduction to energy consumption reduction increases in scenarios 1 to 4, indicating an increase in the climate efficiency of planned renovations. The increase in this indicator is particularly large for scenario 4, indicating that the window replacements implemented in this variant are characterized by high climate efficiency. A significant decrease in RCO_2 is observed for scenario 8, which includes the retrotiffing of the DHW system. Although DHW retrotiffing reduces CO_2 emissions over 30 years, the environmental impact of this retrotiffings very low when considering the ratio of CO_2 emission reduction to energy consumption reduction. A similar effect can be observed in scenario 10a, for which RCO_2 is the only negative value. Scenario 10a involves changing the heat source from a district heating substation to a heat pump. The climate efficiency of this

Table 9
CO_2 emission in all scenarios, including interventions' CO_2 emissions and maintenance' CO_2 emissions during 30-year life cycle.

Scenarios	CO_2 emission in 30 years [kg CO_2]			Share of embodied in the total CO_2 emissions due to retrofitting [%]
	Investments	Operational	Total	
actually	–	1 310 060.1	1 310 060.1	–
Scenario 1	76.44	1 307 756.7	1 307 833.1	0.01
Scenario 2	13 625.32	931 143.9	944 769.2	1.44
Scenario 3	19 460.26	797 239.2	816 699.5	2.38
Scenario 4	33 310.30	633 798.9	667 109.2	4.99
Scenario 5	33 901.35	621 655.8	655 557.2	5.17
Scenario 6	34 660.51	588 046.2	622 706.7	5.57
Scenario 7	40 122.23	519 934.5	560 056.7	7.16
Scenario 8	40 204.74	501 241.8	541 446.5	7.43
Scenario 9	46 693.08	450 240.0	496 933.1	9.40
Scenario 10A	43 675.64	357 931.5	401 607.1	10.88
Scenario 10B	47 426.51	279 177.6	326 604.1	14.52
Scenario 10C	49 356.33	228 506.4	277 862.7	17.76

Table 10
Reduction of CO_2 emission in individual retrotiffing scenarios and CO_2 emission rate related to the implementation of the scenario per unit of final energy saved.

Scenarios	Reduction of CO_2 emissions compared to the current state [kg CO_2]	[%]	CO_2 emission rate related to the implementation of the scenario per unit of final energy saved [kgCO_2/GJ]
Scenario 1	2 226.86	0.17	50.50
Scenario 2	365 290.85	27.88	50.35
Scenario 3	493 360.62	37.66	50.25
Scenario 4	642 950.79	49.08	49.66
Scenario 5	654 502.98	49.96	49.66
Scenario 6	687 353.19	52.47	49.72
Scenario 7	750 003.30	57.25	49.58
Scenario 8	768 613.55	58.67	49.63
Scenario 9	813 126.83	62.07	49.39
Scenario 10A	908 452.91	69.34	39.63
Scenario 10B	983 455.91	75.07	42.03
Scenario 10C	1 032 197.31	78.79	43.54

solution is very low because in this variant, the heat pump is powered solely by electricity from the local grid, which has a negative environmental impact due to the energy mix containing a large share of fossil fuels such as coal. The decrease in RCO_2 in scenario 10a is directly related to the observed decrease in CO_2 emission rate related to the implementation of the scenario per unit of final energy saved (Table 10). At the same time, it can be noted that the use of PV panels (scenario 10b) and PV panels with storage (10c) causes an increase in RCO_2 and this is accompanied by an increase in annual energy savings (Table 8), an increase in the share of embodied CO_2 emissions due to retrofitting (Table 9), and an increase in CO_2 emission rate related to the implementation of the scenario per unit of final energy saved (Table 10).

The literature presents very well the percentage of heat savings and emissions. The absolute emission reduction values reported in most studies to date are significant. To date, the literature has primarily reported percentage-based values of heat savings and emission reduction resulting from building renovations, both with absolute emission reduction values which are significant. In this article, the authors wanted to highlight and using the example of the kindergarten analyzed, propose the RCO_2 indicator, which will allow us to obtain information on the efficiency of the given building retrofit scenario solution in the future. Based on this, the information about the individual intervention scenarios from an emissions reduction perspective is more understandable. In most energy audits, this is not the first option, due to the high investment costs. In the analyzed kindergarten, among the construction options (scenarios 1–9), it is option 4, in accordance with the increasing SPBT value. However, using the RCO_2 indicator, it is the first option among the options regarding the building's thermal insulation. In this article, using the example of the analyzed kindergarten building, the authors propose the RCO_2 indicator as a tool for evaluating the effectiveness of different building retrofit scenarios. The application of this indicator allows for a clearer and more transparent comparison of individual intervention scenarios from the perspective of emission reduction. In standard energy audits, such an approach is rarely prioritized, mainly due to high investment costs. In the analyzed kindergarten, among the considered construction scenarios (1–9), scenario 4 is ranked lower when evaluated using the increasing SPBT criterion. The SPBT criterion is required in the methodology [18] required by Polish legislator. This criterion allows for determining the optimal selection of projects that are included in the scenario. However, when assessed using the RCO_2 indicator, this scenario becomes the most favorable option among the thermal insulation measures considered.

Interestingly, the heat pump scenario shows a negative embodied emission value, which initially appears counterintuitive. This is primarily due to the inclusion of Module D (Table 6) credits related to material recycling (90–95% recovery rates). When these benefits are allocated to future life-cycle stages, the resulting "net-negative" embodied emissions can overshadow the operational burdens.

While such outcomes are methodologically proper under EN 15978, they highlight the need for caution when interpreting negative embodied emissions, as the real-world recovery rates and substitution benefits may vary. A similar effect is observed for PV panels and the energy storage system, where environmental credits approach.but do not exceed. the embodied burdens.

The main strength of this new indicator lies in its independence from energy costs, ensuring that higher values unequivocally represent greater climate efficiency per unit of energy saved. The LCA methodology applied in this study is fully aligned with established standards, focusing on product and operational stages to provide robust and comparable results. While demolition and waste management phases connected with retrofitting (e.g. old windows that were removed) were not included, their omission does not compromise the validity of the findings; rather, it highlights an opportunity for future research to extend the scope of assessment.

In terms of efficiency, the retrotiffing of the DHW system demonstrated a remarkably low embodied emission rate (0.23 kg CO_2/GJ), making it an excellent candidate for low-cost, low-impact intervention.

8.3. *Limitations and future work*

Moreover, we can consider some limitations and gaps regarding the

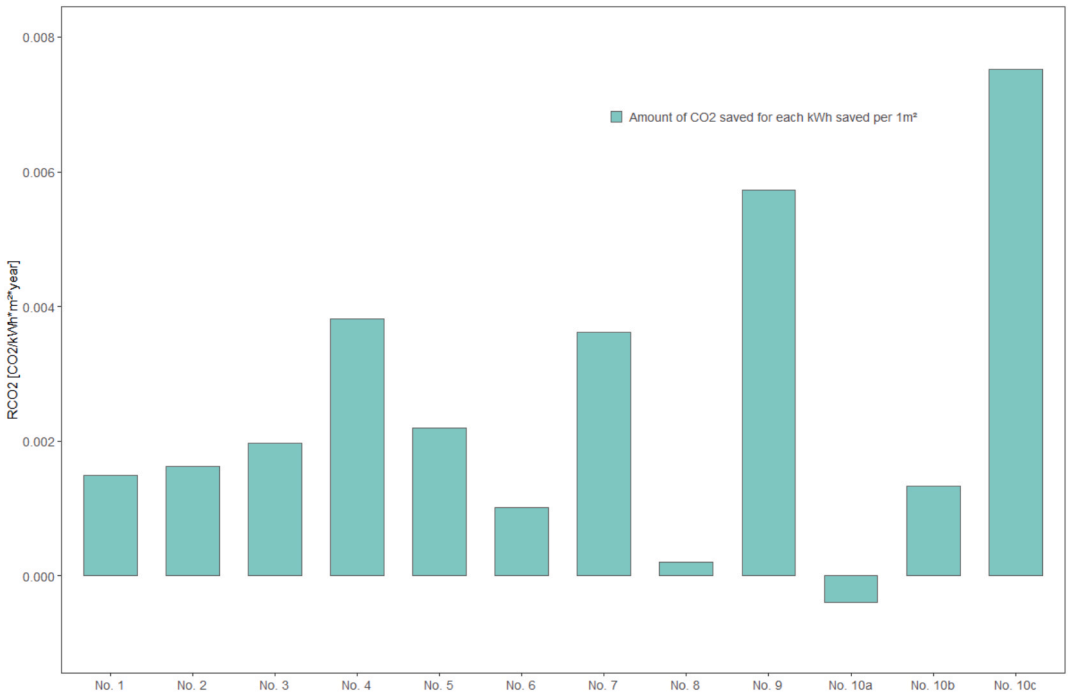

Fig. 15. Values of new proposed CO_2 reduction efficiency indicator – RCO_2 for analyzed retrofitting scenarios.

methodology suggested by standards for LCA analysis, that seem to be better fitted to new constructions than retrofitting interventions. In this LCA analysis for the building retrofit, only the environmental impact of the elements (e.g., windows [55], doors, the heat source) was considered, rather than the full process of removing and replacing the existing ones. This approach is consistent with typical retrofitting LCA methodologies, which focus on comparing the environmental performance of new materials or systems rather than modelling the entire dismantling process. Actual methodology assumes that the existing windows are already part of the building's baseline, and their environmental impact was accounted for at the time of original construction. Our assumptions were in line with [56] where only product and operational stages were considered based on EN 15978:2011 [57] recommendations that *"if there is no previous LCA for the building, impacts from renovations should be treated as a new life cycle (*i.e. *from module A)*".

A critical methodological aspect concerns the scope of the LCA. Following EN 15978, only product (A1–A3) and operational stages (B6) were included, and replacement of existing components was treated as the beginning of a new life cycle. While this approach aligns with standard practice in retrofit LCAs, it excludes dismantling, waste management, and end-of-life processes associated with removed elements that may lead to underestimations of certain embodied impacts.

Existing LCA frameworks are optimized primarily for new construction and do not fully capture retrofit-specific processes. Future work should address these gaps by extending system boundaries and improving modelling of end-of-life pathways, thereby enabling more comprehensive assessments of building retrotiffing strategies, especially in regions dominated by aging building stock. Our perspective aligns with the findings of Fahlstedt et al. [17], who noted that excluding replacement phases in LCA may lead to an underestimation of environmental impacts. It is important to note that in the case of retrofitting existing buildings, the process generates waste from the removal of old windows, doors, sanitary installations, and other components. The demolition and waste disposal phases also contribute to CO_2 emissions. However, our LCA did not include the dismantling and disposal of existing building elements. Additional reason to such approach is often the lack of reliable historical data on the materials, technologies, and emissions associated with the production and use of these original components. Summarizing, a comprehensive environmental assessment would require detailed information about the earlier life cycle stages of the replaced elements, including their material composition, manufacturing processes, and operational impacts.

Overall, the findings confirm that while, envelope insulation remains crucial for long-term emission reductions but may involve higher upfront carbon costs. By contrast, renewable energy systems, particularly when coupled with storage, exhibit the highest carbon efficiency per unit of energy saved, supporting their integration into deep retrotiffing scenarios. us, a balanced retrofit strategy should account for both operational and embodied emissions, aiming to optimize the carbon payback period. However, future work should focus on expanding LCA boundaries to include maintenance, end-of-life scenarios, and user behavior, which significantly influence real-world performance. Undouble, findings of this study support evidence-based decision-making in sustainable building renovation. It proposes LCA metrics that should be taken into account on early-stage planning for climate-resilient infrastructure.

9. Conclusions

This study assessed the environmental performance of a range of retrofit interventions for an existing kindergarten building located in a cold temperate climate, examining both embodied and operational CO_2 emissions over a 30-year life cycle. The results confirm the dominant role of operational emissions in the building's overall carbon profile, while embodied emissions vary widely depending on the intervention type and material intensity. Although envelope-related measures, such as external wall insulation, flat roof insulation, and window replacement, achieve substantial absolute reductions in CO_2 emissions, their performance per unit of energy saved underscores the need to account for the carbon costs of materials when prioritizing retrofit pathways.

To support decision-making, the study introduces the RCO_2 indicator, which expresses CO_2 emission reduction as a function of energy savings and usable floor area. This metric allows for cross-comparison of retrofit strategies independent of financial considerations or energy prices. The application of RCO_2 highlights the superior climate efficiency of renewable energy interventions, particularly the combined use

of a modern heat source, PV installation, and energy storage. These solutions deliver the highest emission reduction per unit of energy saved, reinforcing their strategic importance in deep retrotiffing scenarios under decarbonization targets. Heating system retrotiffing and window replacement also demonstrate strong and consistent performance across the assessed criteria. The proposed RCO_2 indicator contributes a practical and intuitive tool for early-stage planning, enabling stakeholders to identify interventions that deliver the highest climate benefits relative to their energy savings.

The findings of this study offer several implications for policymakers, local authorities, and practitioners. Energy audits and retrotiffingguidelines should incorporate carbon-based indicators such as RCO_2 to complement economic metrics. This would enable more climate-oriented decision-making in early planning phases and avoid sub-optimal choices driven solely by payback time.

Limitations of the presented analysis are given by the use of fixed emission factors for electricity and district heating over a 30-year period. In fact, as is well known, the emissions of carbon dioxide - connected to the use of electricity change from time to time. Moreover, these values are strongly dependent on how (and thus, where) electricity is produced [63], and may be influenced by the transition to decarbonization and a more sustainable energy mix. However, a recent paper has investigated the use of dynamic emission factors in LCA assessments, showing variabilities within a limited range [64].

On the contrary, the introduction of the new RCO_2 indicator allows one to overcome another limitation of the traditional approach to life cycle analysis. In fact, the role of climate conditions may also affect the results of the traditional approach to life cycle analysis. Over the last 50 years, the energy consumption of buildings has been shown to have changed in response to actual climate data [65]. In the present paper, we used energy consumption information coming from the utility bills of the last years. If such analysis is used to estimate future scenarios, the approach should be expanded to account for the role of variations in external conditions resulting from climate change. In this framework, indeed, the new RCO_2 indicator, which is defined as the CO_2 emission reduction over the energy consumption reduction (per unit of usable building area), allows comparison between building retrofitting scenarios independently of increasing or decreasing energy consumption due to climate systematic variations.

Finally, the choice of public-sector buildings (e.g. kindergartens, schools, universities) represents a strategic opportunity: applying combined envelope improvements and renewable technologies can support compliance with EU directives on nearly zero-energy and zero-emission buildings. while simultaneously serving an important educational function by exposing students, staff, and the wider community to visible examples of sustainable technologies and climate-responsible practices. Such buildings can act as demonstrators of the green transition, fostering environmental awareness and strengthening societal support for long-term decarbonization efforts.

CRediT authorship contribution statement

Elżbieta Broniewicz: Writing – original draft, Validation, Software, Methodology, Investigation, Formal analysis, Data curation, Conceptualization. **Piotr Rynkowski:** Writing – original draft, Visualization, Validation, Software, Methodology, Investigation, Formal analysis, Data curation, Conceptualization. **Beata Sadowska:** Writing – original draft, Visualization, Validation, Methodology, Investigation, Formal analysis, Data curation. **Anna Justyna Werner-Juszczuk:** Writing – original draft, Visualization, Validation, Methodology, Investigation, Formal analysis, Data curation. **Eugenia Rossi di Schio:** . **Paolo Valdiserri:** Writing – review & editing, Investigation, Data curation. **Maciej Kłopotowski:** Visualization, Investigation, Data curation. **Bożena Babiarz:** Writing – review & editing, Investigation, Data curation. **Alicja Siuta-Olcha:** Writing – review & editing, Investigation, Data curation. **Tomasz Cholewa:** Writing – review & editing, Investigation, Data curation. **Dorota Anna Krawczyk:** Writing – review & editing, Writing – original draft, Project administration, Methodology, Funding acquisition, Formal analysis, Data curation, Conceptualization.

Declaration of competing interest

The authors declare that they have no known competing financial interests or personal relationships that could have appeared to influence the work reported in this paper.

Acknowledgments

The research leading to these results was conducted as a part of the project “VIA CARPATIA Universities of Technology Network named after the President of the Republic of Poland Lech Kaczynski”, the Minister of Science, contract no.MEiN/2022/DPI/2575, MEiN/2022/DPI/2577, MEiN/2022/DPI/2578, action entitled “ISKRA—building inter-university research teams”.

Appendix

ANNEX A.

Case study Background

In Poland, World War II caused widespread destruction in many cities, leading to a significant need for reconstruction. Beginning in the 1950 s, an intensive period of urban rebuilding took place across the country. New residential districts were developed along with the necessary public infrastructure. including schools, kindergartens, health centers, and shops. At the time, design standards were in force for kindergartens, specifying plot sizes, building shapes, and window surface area requirements. As a result, a large number of kindergarten buildings with standardized architectural forms were constructed throughout Poland. According to building standards in force in Poland during the 1970 s and 1980s [58,59,60], kindergartens constructed in residential neighbourhoods were typically designed to accommodate four groups of children aged 3 to 6 years. These facilities were required to be located on plots of land measuring between 0.4 and 0.48 ha, within housing estates, ensuring accessibility within a specified walking distance – generally assumed to be several minutes for young children. For each group, a dedicated activity room was required, proportionate to the group size (typically 30 children per group), with a minimum area of 60 m^2. These rooms were to be oriented in a direction that ensured appropriate exposure to sunlight, in line with the prevailing standards for natural lighting and comfort in educational spaces.

This study was conducted in Bialystok, city located in northeastern Poland, where a total of 45 kindergartens were built between 1950 and 1990 – the period during which these normative regulations were in effect. These buildings represent over 40% of all currently operating kindergartens in the city [20]. The selection of the kindergarten building for this analysis was based on two criteria. The first was the typicality of the building, to enable the extrapolation of the findings to similar facilities across the country. The second was the lack of previous retrotiffing, in order to identify the optimal retrofit scenario based on an LCA of proposed interventions.

Building Description

Ultimately, Public Kindergarten No. 68, was selected for analysis. The building was constructed in 1984 and it represents a group of kindergartens with the most favorable spatial characteristics, as classified by Krawczyk et al. [25], including: a large, independent plot exceeding 1,000 m^2, a detached building or a separated ground-floor section of a residential block, a sizable playground, and well-developed greenery. The facility currently serves 143 children and 30 staff members.

The kindergarten is situated on a rectangular plot of approximately 4,500 m^2, with a length-to-width ratio close to 2:1 (see Fig. A1). The building footprint is about 474 m^2 (approximately 36.60 m by 12.90 m), occupying around 10% of the total plot area. The building height is approximately 8.40 m.

The main axis of the plot runs from northeast to southwest. The kindergarten building is located centrally and oriented perpendicularly to this axis, creating two green zones on either side, primarily used as children's playgrounds. The entire plot is surrounded by rows of deciduous trees (mainly lindens and Douglas firs) approximately 15 m high and 35–40 years old. These trees provide a natural buffer between the kindergarten and the surrounding residential blocks and streets but also contribute to substantial shading of the plot and the building itself.

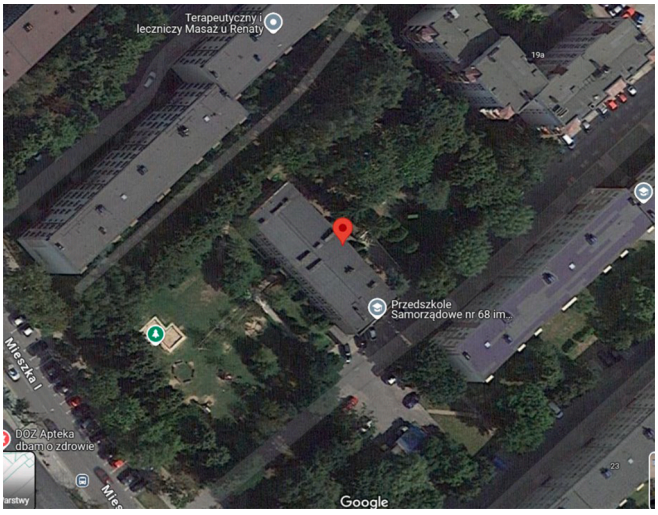

Fig. A1. Location of the object of the study [61,62].

The kindergarten building (Fig.A1-2) has two above-ground storeys and a basement. Its main entrance is located on the northeast side of the building. The usable floor area is estimated as 1,159.55 m^2, while its heated volume: 3,385.9 m^3. The building features a cuboidal form with a flat roof, and its facade is articulated by continuous rows of identical large windows that emphasize each storey. These windows have a characteristic configuration consisting of four outward-tilting sashes arranged in two horizontal bands, with three vertically opening sashes between them.

Originally, the building included four classrooms for different age groups (from 3 to 6 years), each with an area of approximately 67 m^2. The rooms were symmetrically distributed – two on the ground floor and two on the first floor, all located on the southwest-facing side to ensure optimal solar exposure. In 2017, a fifth classroom was added by adapting a room previously used for shared activities (e.g., holiday events or group celebrations). However, this classroom is less favorably oriented, with windows facing northeast, thus receiving limited direct sunlight.

Each classroom is equipped with four identical windows measuring 245 × 230 cm, providing approximately 22.5 m^2 of glazing, which corresponds to roughly 33% of the classroom floor area.

Fig. A2. Elevation views of the analyzed building [own photos]

The basement walls are made of large-block prefabricated elements ("Cegła Żerańska"), with a 3 cm layer of mineral wool insulation, faced with 6.5 cm thick perforated bricks. The above-ground walls were constructed using a combination of prefabricated "Cegła Żerańska" blocks and 18 cm thick aerated concrete blocks. The vestibule walls are made of traditional masonry. The inter-storey floor structure consists of prefabricated elements made from "Cegła Żerańska". The ventilated flat roof comprises 10 cm thick corrugated slabs supported by the prefabricated floor structure through openwork partition walls. The lower side of the roof is insulated with 7 cm thick insulating mats. The canopy over the vestibule has a reinforced concrete structure with a thickness of 8 cm, topped with a 2 cm cement screed and two layers of roofing felt. The window joinery is made of PVC, while the doors are a combination of PVC and wooden elements [26].

ANNEX B

The assumptions for LCA (each analyzed scenario) – LCA for Expert (Sphera, v.10.9.3.0) database.

No	Intervention	Material/equipment	Unit	Value	End of Life	Source
1	Insulation of the canopy over the vestibule	Expanded Polystyrene (EPS) Foam (25 kg/m^3), 13 cm	m^{2}kg	2.98.6	co-incineration of polystyrene waste in an incinerator	Sphera Database, ULLMANN: Foamed Plastics, 1999–2023
		Bitumen sheets G 200 S45 kg/m^2	Kg	14.3	thermal treatment of hazardous waste	Sphera Database, The Bitumen Roofing Industry – A Global Perspective
		Asphalt binder0.3 kg/m^2	kg	4.3	thermal treatment of hazardous waste	Sphera Database, BAFU: Anthropogene VOC-Emissionen – Schweiz 1998 und 2001, Bern, 2004
2	External walls insulation	ETIC (Adhesion and coating, silicone resin plaster) 12–13.5 kg/m^3	m^2	640	construction waste dumping	Sphera Database, Eco profiles of production systems for silicones, 2002
		Expanded Polystyrene (EPS) 15 kg/m^3	kg	1,635	co-incineration of polystyrene waste in an incinerator	Sphera Database, ULLMANN: Foamed Plastics, 1999–2023
3	Flat roof insulation	Glass wool insulation, 24 cm, 30–45 kg/m^3	m^{2}kg	431.93,120	mineral wool in waste incineration plant	Sphera Database, AUB-Deklaration Rockwool
4	Windows' repacement U = 0.9 Wm^{2}K	Window glass simple	kg	1,138.6	disposal of glass (landfill/incineration)	Sphera
		Metal fitting for double casement windows	kg	627	pl: ferro metals in waste incineration plant	Sphera
		Polyvinylchloride injection moulding part (PVC)	kg	1,881	PVC in waste incineration plant. recycling	Plastic Europe
5	Doors' replacementU = 1.3 Wm^{2}K	Window/door glass simple	kg	67.6	disposal of glass (landfill/incineration	Sphera
		Metal fitting	kg	24	pl: ferro metals in waste incineration plant	Sphera
		Polyvinylchloride injection moulding part (PVC)	kg	18.03	PVCin waste incineration plant	Plastic Europe

(*continued on next page*)

(*continued*)

No	Intervention	Material/equipment	Unit	Value	End of Life	Source
6	Basement walls insulation (above ground)	ETIC (Adhesion and coating. silicone resin plaster) 13 cm, 20–50 kg/m^3	m^2	74.53	construction waste dumping	Sphera Database, Eco profiles of production systems for silicones, 2002
		Expanded Polystyrene (EPS), 25 kg/m^3	kg	242.5	co-incineration of polystyrene waste	Sphera Database, ULLMANN: Foamed Plastics, 1999–2023
7	Basement wall insulation (in the ground)	Extruded polystyrene (XPS) 13 cm, 20–50 kg/m^3	m^2kg	156.25650	co-incineration of polystyrene waste	Sphera Database,
		Asphalt binder	kg	1,563	thermal treatment of hazardous waste	Sphera Database, BAFU: Anthropogene VOC-Emissionen – Schweiz 1998 und 2001, Bern, 2004
8	DHW retrotiffing	Polyurethane flexible foam (PU), density 18 to 25 kg/m^3 – hardness 2.5 to 4 kPa	kg	19.2	polyurethane hard foam (Pipe insulation); End of Life	Sphera Database
		Red brass part	kg	0.6	Red brass recycling	Sphera Database
9	CH retrotiffing	Polyurethane flexible foam (PU). density 35 to 40 kg/m^3 hardness 3.8 to 5 kPa	kg	68.3	polyurethane hard foam (Pipe insulation); End of Life	Sphera Database
		Polyvinyl chloride film (PVC) 20–30 mm	kg	0.007	polyurethane hard foam (Pipe insulation); End of Life	Plastic Europe
		Red brass part	kg	60.7	Red brass recycling	Sphera Database
		Radiators	kg	1,722	Ferro metals on landfill	Sphera Database, VDI 2067
10A	Replacement of the existing district heating substation with an air-source heat pump	Electric heat pump 14 kW air/water 5.7 x 2 = 11.4	kW	80	Electric heat pump 14 kW air/water; End of Life + Credits	Sphera Database, VDI 2067, BUDERUS 2007, KAUT 2008
10B	Installation of a new air-source heat pump in conjunction with a photovoltaic (PV) system, enabling partial on-site electricity generation	Electric heat pump 14 kW air/water 5.7 x 2 = 11.4	kW	80	Electric heat pump 14 kW air/ waterEnd of Life + Credits	Sphera Database, VDI 2067, BUDERUS 2007, KAUT 2008
		Electricity from photovoltaic PL	kWh/rok	4,396.9	End of Life	Sphera Database
10C	Implementation of a new air-source heat pump combined with both a photovoltaic system and an electricity storage system, enabling increased self-sufficiency and energy resilience	Electric heat pump 14 kW air/water 5.7 x 2 = 11.4	kW	80	Electric heat pump 14 kW air/water; End of Life + Credits	Sphera Database, VDI 2067, BUDERUS 2007, KAUT 2008
		Electricity from photovoltaic PL	kWh/rok	4,396.9	End of Life	Sphera Database
		Lithium iron phosphate battery	kg	1000	Steel scrap (EoL phase) 369.6 kg, Copper scrap (>95% Cu content) [Waste for recovery] 148.3 kg, Aluminium scrap [Waste for recovery] 175.4 kg,Plastic (unspecific) [Waste for recovery] 372.4 kg	Sphera Database
		Electricity from renewable sources	kWh/rok	2,829.2	Credits	

Data availability

Data will be made available on request.

References

[1] European Union. Directive (EU) 2023/1791 of the European Parliament and of the Council of 13 September 2023 on energy efficiency and amending Regulation (EU) 2023/955 (recast) (Text with EEA relevance). Off. J. Eur. Union. L 231, 20.9.2023.

[2] European Commission. Making our homes and buildings fit for a greener future – Buildings. European Commission Factsheet. https://commission.europa.eu/document/download/f4e5e0c4-d767-4f4c-a25c-045e9f877229_en?filename=Buildings_Factsheet_EN_final.pdf [Accessed 29 June 2025].

[3] European Union. Directive (EU) 2023/2413 of the European Parliament and of the Council of 18 October 2023 amending Directive (EU) 2018/2001, Regulation (EU) 2018/1999 and Directive 98/70/EC as regards the promotion of energy from renewable sources, and repealing Council Directive (EU) 2015/652. Off. J. Eur. Union. L 2023/2413, 31.10.2023.

[4] European Commission. A RetrotiffingWave for Europe – Greening our buildings, creating jobs, improving lives. Communication from the Commission to the European Parliament, the Council, the European Economic and Social Committee and the Committee of the Regions. COM(2020) 662 final. https://eur-lex.europa.eu/legal-content/EN/TXT/?uri=CELEX%3A52020DC0662 [Accessed 29 June 2025].

[5] T. Terlouw, C. Bauer, L. Rosa, M. Mazzotti, Life cycle assessment of carbon dioxide removal technologies: a critical review, Energy Environ. Sci. 14 (2021) 1701–1721, https://doi.org/10.1039/D0EE03757E.

[6] J. Famiglietti, T.H. Amini, A. Dénarié, M. Motta, Developing a new data-driven LCA tool at the urban scale: the case of the energy performance of the building sector, Energy Convers. Manag. 256 (2022) 115389, https://doi.org/10.1016/j.enconman.2022.115389.

[7] R. Dylewski, J. Adamczyk, The environmental impacts of thermal insulation of buildings including the categories of damage: a polish case study, J. Clean. Prod. 137 (2016) 878–887, https://doi.org/10.1016/j.jclepro.2016.07.172.

[8] E. Makhmudov, A. Zavaleeva, I. Zavaleev, A. Berdimurodov, Life cycle analysis of a retrotiffingproject for old housing in Tashkent to reduce greenhouse gas emissions, E3S Web Conf. 574 (2024) 05007, https://doi.org/10.1051/e3sconf/202457405007.

[9] D. González-Prieto, Y. Fernández-Nava, E. Marañón, M.M. Prieto, Environmental life cycle assessment based on the retrofitting of a twentieth-century heritage building in Spain. with electricity decarbonization scenarios, Building Research & Information. 49 (8) (2021) 859–877, https://doi.org/10.1080/09613218.2021.1952400.

[10] J. Adamczyk, R. Dylewski, Ecological and economic benefits of the "medium" level of the building thermo-: a case study in Poland, Energies 13 (17) (2020) 4509, https://doi.org/10.3390/en13174509.

[11] F. Asdrubali, I. Ballarini, V. Corrado, L. Evangelisti, G. Grazieschi, C. Guattari, Energy and environmental payback times for an NZEB retrofit, Build. Environ. 147 (2019) 461–472, https://doi.org/10.1016/j.buildenv.2018.10.047.

[12] Alessio Mastrucci. Antonino Marvuglia. Enrico Benetto. Ulrich Leopold: A spatio-temporal life cycle assessment framework for building retrotiffingscenarios at the

urban scale. Renewable and Sustainable Energy Reviews. Volume 126. 2020. 109834. ISSN 1364-0321. https://doi.org/10.1016/j.rser.2020.109834.
[13] J. Sierra-Pérez, B. Rodríguez-Soria, J. Boschmonart-Rives, X. Gabarrell, Integrated life cycle assessment and thermodynamic simulation of a public building's envelope renovation: conventional vs, Passivhaus Proposal. Appl. Energy. 212 (2018) 1510–1521, https://doi.org/10.1016/j.apenergy.2017.12.101.
[14] A. Stephan, R.H. Crawford, K. de Myttenaere, Towards a comprehensive life cycle energy analysis framework for residential buildings, Energ. Buildings 55 (2012) 592–600.
[15] M. Leichter, C. Piccardo, Assessing life cycle sustainability of building retrotiffingand reconstruction: a comprehensive review of case studies and methods, Build. Environ. 262 (2024) 111817, https://doi.org/10.1016/j.buildenv.2024.111817.
[16] A. Vilches, A. Garcia-Martinez, B. Sanchez-Montanes, Life cycle assessment (LCA) of building refurbishment: a literature review, Energy Build. 135 (2017) 286–301.
[17] O. Fahlstedt, R.F. Nygaard, A. Temeljotov-Salaj, L. Huang, R.A. Bohne, Building renovations and life cycle assessment – a scoping literature review, Renew. Sustain. Energy Rev. 203 (2024) 114774, https://doi.org/10.1016/j.rser.2024.114774.
[18] Polish Ministry of Infrastructure. Regulation of the Minister of Infrastructure of 17 March 2009 on the Detailed Scope and Forms of the Energy Audit and Part of the Energy Audit, Audit Card Templates, as well as the Algorithm for Assessing the Profitability of a Thermo Project; Polish Ministry of Infrastructure: Warsaw, Poland, 2009. Available online: https://isap.sejm.gov.pl/isap.nsf/DocDetails.xsp?id=WDU20090430346 (accessed 26 May 2025).
[19] Polish Ministry of Infrastructure. Regulation of the Minister of Infrastructure of 27 February 2015 on the Methodology for Calculating the Energy Performance of a Building or Part of a Building and Energy Performance Certificates. J. Laws Repub. Pol. Item 376. Available online: http://prawo.sejm.gov.pl/isap.nsf/DocDetails.xsp?id=WDU20150000376 (accessed 26 May 2025).
[20] D.A. Krawczyk, A. Werner-Juszczuk, B. Sadowska, P. Rynkowski, A. Siuta-Olcha, B. Babiarz, A. Święcicki, R. Stachniewicz, T. Cholewa, L. Lichołai, J. Krasoń, P. Miąsik, M. Bocian, M. Kłopotowski, D. Gawryluk, New method of retrofitting of kindergartens resulting in increase of energy self-sufficiency, Energy Build. 336 (2025) 115595, https://doi.org/10.1016/j.enbuild.2025.115595.
[21] Institute of Meteorology and Water Management (IMGW). Dane meteorologiczne – stacje synoptyczne. Available online: https://danepubliczne.imgw.pl/data/dane_pomiarowo_obserwacyjne/dane_meteorologiczne/terminowe/synop/ (accessed 29 June 2025).
[22] European Commission Joint Research Centre (JRC). PVGIS – Photovoltaic Geographical Information System. https://re.jrc.ec.europa.eu/pvg_tools/en/ (accessed 29 June 2025).
[23] ISO. ISO 14040:2006+A1:2020 – Environmental Management – Life Cycle Assessment – Principles and Framework. Geneva: International Organization for Standardization; 2020.
[24] ISO. ISO 14044:2006+A2:2020 – Environmental Management – Life Cycle Assessment – Requirements and Guidelines – Amendment 2. Geneva: International Organization for Standardization; 2020.
[25] D.A. Krawczyk, M. Kłopotowski, D. Gawryluk, et al., Evaluation of accessibility of kindergarten playgrounds and outdoor green areas in polish cities, Urban Des. Int. (2024), https://doi.org/10.1057/s41289-024-00254-3.
[26] Sadowska B., Sarosiek B.W. Audyt energetyczny budynku Przedszkola. Białystok: NAPE S.A.; 2024 (Energy audit of the kindergarten building - in Polish).
[27] Polish Ministry of Transport, Construction and Maritime Economy. Regulation of the Minister of Transport, Construction and Maritime Economy of 5 July 2013 on the Technical Conditions that Buildings and Their Location Should Satisfy. Warsaw: Polish Ministry of Transport, Construction and Maritime Economy; 2015.
[28] EN ISO 52010 Energy performance of buildings — External climatic conditions Part 1: Conversion of climatic data for energy calculations.
[29] Werner-Juszczuk A., Krawczyk D.A., et al. Assessment of the possibility of locating photovoltaic panels in the area around, presented on 10th International Conference on Advances on Clean Energy Research 2025, in press.
[30] B. Dai, Y. Hao, S. Liu, D. Wang, R. Zhao, X. Wang, J. Liu, F. Zong, T. Zou, Hybrid CO air source heat pump system integrating vapor injection and mechanical subcooling technology for space heating of global application: Life cycle techno-energy-enviro-economics assessment, Energy Convers. Manag. 271 (2022) 116324, https://doi.org/10.1016/j.enconman.2022.116324.
[31] A. Santecchia, R. Castro-Amoedo, T.-V. Nguyen, I. Kantor, P. Stadler, F. Maréchal, The critical role of electricity storage for a clean and renewable European economy, Energy Environ. Sci. 16 (2023) 5350–5370, https://doi.org/10.1039/D3EE02768F.
[32] Stiebel-Eltron. Available online: https://www.stiebel-eltron.pl/ (accessed 29 June 2025).
[33] Segensolar. Monocrystalline PV panel Jinko Tiger Neo 480 Wp n-type (black frame) with junction boxes. Available online: https://www.segensolar.pl/product/jinko/pv-panel-jinko/monocrystalline-pv-panel-jinko-jinko/tiger-neo-480wp-n-type-mono-z-wtyczkami-jk03-czarna-ramka/ (accessed 29 June 2025).
[34] Columbus Energy. Energy storage 100 kWh. Available online: https://columbusenergy.pl/magazyn-energii-100-kwh/ (accessed 29 June 2025).
[35] NRG Storage. Energy storage 100 kWh. Available online: https://nrgstorage.pl/magazyn-energii-100-kwh/ (accessed 29 June 2025).
[36] Ch. Gu, H. Gu, M. Gong, J. Blackadar, A Case Study on the Impact of Transportation of Mass Timber Products on the Cradle-to-Gate LCA results for an Institutional building, Recent Progress in Materials. 4 (2022) 1. https://doi.org/10.21926/rpm.2203014.
[37] S. Ge, X. Zhang, X. Zhang, Integration of BIM and LCA: a system to predict and optimise embodied carbon for prefabricated buildings, HKIE Trans. 30 (3) (2024) 44–55. https://doi.org/10.33430/V30N3THIE-2022-0052.
[38] T. Chao, K.W. Tan, Quantification of Embodied Carbon (EC) for Residential Development Project, Civil and Environmental Engineering 21 (2) (2025) 1193–1204, https://doi.org/10.2478/cee-2025-0088).
[39] Search Life Cycle Assessment Datasets, https://lcadatabase.sphera.com/, (access: May, 2025).
[40] CEN/TC 350. EN 15804:2012+A2:2019 – Sustainability of construction works – Environmental product declarations – Core rules for the product category of construction products. Brussels: CEN; 2019.
[41] Manufacturer datasheets available at http://systemyocieplen.pl/wiedza_detail.php?id=141 (access: 26.05.2025).
[42] Manufacturer datasheets available at https://oknotest.pl/poradnik-okienny/ile_wazy_szyba_ile_wazy_okno (access: 26.05.2025).
[43] Manufacturer datasheets available at https://kan-therm.com/pl (access: 02.06.2025).
[44] Manufacturer datasheets available at https://www.purmo.com/pl-pl (access: 28.05.2025).
[45] Manufacturer datasheets available at https://www.danfoss.com/pl-pl/ (access: 28.05.2025).
[46] G. Naumann, E. Schropp, M. Gaderer, Life cycle assessment of an air-source heat pump and a condensing gas boiler using an attributional and a consequential approach, Procedia CIRP 105 (2022) 351–356, https://doi.org/10.1016/j.procir.2022.02.058.
[47] DRIVERS TO HEAT PUMP ADOPTION BY EUROPEAN HOUSEHOLDS. DAIKIN EUROPE. January 2024. https://www.daikin.eu/en_us/solutions/for-your-home/environmental-impact-of-heat-pumps.html.
[48] Report: Life Cycle Inventories and Life Cycle Assessments of Photovoltaic Systems 2020.
[49] Publications: IEA PVPS Task 12 - https://iea-pvps.org/research-tasks/pv-sustainability/ Frischknecht. L. Krebs (Ed.). Life Cycle Inventories and Life Cycle Assessments of Photovoltaic Systems. PV Power System Task. Report IEA-PVPS T12-19:2020. 2021.
[50] https://iea-pvps.org/wp-content/uploads/2020/12/IEA-PVPS-LCI-report-2020.pdf.
[51] Zhu. Lingyun. and Ming Chen. 2020. "Research on Spent LiFePO4 Electric Vehicle Battery Disposal and Its Life Cycle Inventory Collection in China" International Journal of Environmental Research and Public Health 17. no. 23: 8828. https://doi.org/10.3390/ijerph17238828.
[52] Manufacturer datasheets available https://www.enea.pl/sites/default/files/2025-05/Charakterystyka%20systemu.pdf access: 02.06.2025).
[53] Polish National Inventory Report 2024. Heating Values and CO_2 Emission Factors in 2022 for Reporting under the Emissions Trading System for 2025; KOBiZE: Warsaw, Poland, 2025. Available online: https://www.kobize.pl (accessed on 26 May 2025). (In Polish).
[54] https://re.jrc.ec.europa.eu/pvg_tools/en/) (access: 20.04.2025).
[55] Liza Saallstrom Eriksson and Sofia Lidelow. Maintaining or replacing a building's windows: a comparative life cycle study International Journal of Building Pathology and Adaptation ISSN: 2398-4708. Published by Emerald Publishing Limited.
[56] Poland's National Inventory Report 2024. Heating Values and CO2 Emission Factors in 2022 for Reporting under the Emissions Trading System for 2025; KOBiZE: Warsaw, Poland, 2025. Available online: https://www.kobize.pl (accessed on 26 May 2025). (In Polish).
[57] EN 15978:2011 EN 15978:2011 Sustainability of construction works - Assessment of environmental performance of buildings - Calculation method.
[58] Korzeniewski W. (1981). Poradnik projektanta budownictwa mieszkaniowego. Warszawa. Arkady (book in Polish).
[59] Zarządzenie nr 9 Ministra Gospodarki Terenowej i Ochrony Środowiska z dnia 29 stycznia 1974 r. w sprawie wskaźników i wytycznych urbanistycznych dla terenów mieszkaniowych w miastach (Dz. Bud. Nr 2, poz. 2). (in Polish).
[60] MAGTOŚ. Projekt normatywu urbanistycznego. December 1975. (in Polish).
[61] Google Maps; location: 53.13395° N, 23.19252° E.
[62] GIS Białystok Miejski System Informacji Przestrzennej - Serwis publiczny (GIS Białystok Municipal Spatial Information System - Public service https://gisbialystok.pl/) (access: 02.03.2025).
[63] P. Valdiserri, V. Ballerini, E.R. di Schio, Interpolating functions for CO2 emission factors in dynamic simulations: the special case of a heat pump, Sustainable Energy Technol. Assess. 53 (2022) 102725.
[64] Müller, A., & Wörner, P. (2019, August). Impact of dynamic CO2 emission factors for the public electricity supply on the life-cycle assessment of energy efficient residential buildings. In IOP Conference Series: Earth and Environmental Science (Vol. 323, No. 1, p. 012036). IOP Publishing.
[65] Ballerini, V., Rossi di Schio, E., & Valdiserri, P. (2025). On the impact of climate change on the thermal energy demand for a building: an analysis based on 50 years of meteorological data. Energy, Ecology and Environment, 1-19.